Analytic Quantum Chromodynamics: An Exact, Finite, Non-Perturbative, Gauge-Invariant, Realistic Model of QCD, with A Particular Choice of Renormalization with Applications to High Energy Elastic Proton-Proton Scattering.

by

Peter H. Tsang

Submitted to the Department of Physics
in partial fulfillment of the requirements for the degree of
Doctor of Philosophy
at
BROWN UNIVERSITY
May 2016

Author .....
Department of Physics
May 1, 2016

Certified by .....
Herbert M. Fried
Professor
Thesis Supervisor

Certified by .....
Chung-I Tan
Professor
Thesis Committee

Certified by .....
Antal Jevicki
Chairman, Department Committee on Graduate Theses
Thesis Committee

Accepted by .....

Analytic Quantum Chromodynamics: An Exact, Finite, Non-Perturbative, Gauge-Invariant, Realistic Model of QCD, with A Particular Choice of Renormalization with Applications to High Energy Elastic Proton-Proton Scattering.

by

Peter H. Tsang

Submitted to the Department of Physics
on May 1, 2016, in partial fulfillment of the
requirements for the degree of
Doctor of Philosophy

Abstract

A new non-perturbative, gauge-invariant, exact, finite model of quantum chromodynamics, with a particular choice of renormalization is applied to high energy elastic pp-scattering. Gauge invariance is insured by explicit cancellations of all gauge dependent gluon propagators. The result is the entire infinite sum of all gluon exchanges between two quarks/(anti)quarks.

With a particular choice for renormalization, this model is tested against hadron elastic scattering at ISR energies with favorable results. The differential cross- section deduced from this model displays a diffraction dip that compares very well with those of experiments. Calculation of infinite loop chains under our renormalization scheme fits experimental data rather favorably. Extension to total scattering cross-section is expected.

Thesis Supervisor: Herbert M. Fried
Title: Professor

Thesis Committee: Chung-I Tan
Title: Professor

Thesis Committee: Antal Jevicki
Title: Chairman, Department Committee on Graduate Theses

This dissertation by Peter H. Tsang is accepted in its present form
by the Department of Physics as satisfying the
dissertation requirement for the degree of Doctor of Philosophy.

Professor Herbert M. Fried .....
Advisor
Professor of Physics

Recommended to the Graduate Council

Professor Antal Jevicki .....
Reader
Professor of Physics

Professor Chung-I Tan .....
Reader
Professor of Physics

Approved by the Graduate Council

Prof. Peter M. Weber .....
Dean of the Graduate School

Curriculum Vitae(iv)

Peter H. Tsang
(US Citizen) Address: 96-11 69th Ave, Forest Hills, NY 11375, USA
peter_tsang@brown.edu, qcd@brown.edu, phtsang@alum.mit.edu, higgsboson@gmail.com

Birth place: Kowloon, Hong Kong

EDUCATION:

Bronx High School of Science - New York City (during High School junior year and senior year, audited courses and received A's at Columbia University's Physics and Math department.)

Massachusetts Institute of Technology

B.S. Physics, 1997 (Nuclear Theory: Energy Statistics in Stadium Billiard - Thesis Advisor Prof. Michel Baranger)

Brown University

M.S. Physics, 2005

Ph.D (expected 2016). Physics, Thesis Advisor - Prof. Herbert M. Fried.

PUBLICATIONS:

N. Garcia, J.H. Li, W. Polkosnik, T.D. Cheung, P.H. Tsang, A.A. Lisyansky, A.Z. Genack

Influencing the approach to the localization threshold. Physica B: Condensed Matter, vol 175, 1991. 9-16.

Peter H. Tsang, Guanglai Li, Yves V. Brun, L. Ben Freund, and Jay X. Tang, "Adhesion of single bacterial cells in the micronewton range", Proceedings of the National Academy of Sciences. vol. 103 no. 15. 2006. (122 citations) This work received international news coverage, including: Science Journals:

Nature 440, 1119 (27 April 2006): `http://www.nature.com/nature/journal/v440/n7088/full/4401119a.html`.

NBC News: `http://www.nbcnews.com/id/12389963/ns/technology_and_science-science/t/bacteria-make-worlds-strongest-glue/#.VfnLkLyi6-I`. Wired: `http://archive.`

wired.com/techbiz/media/news/2006/04/70692.

Science News, Discovery Magazine. Radio/TV: NPR News, CCTV (Chinese), BBC News, Radio Canada. Newspapers: Fox News, CBC (Canada), NRC.NL (Dutch). Websites: Yahoo Top News, NSF.gov, NIH GMS, Wired magazine

H.M.Fried, P.H.Tsang, Y.Gabellini, T. Grandou, Y.-M.Sheu, An Exact, Finite, Gauge-Invariant, Non-Perturbative Model of QCD Renormalization, Annals of Physics. 12/2014; 359. arXiv:1412.2072.

H.M.Fried. P.H.Tsang. A physical version of the QCD confinement scale(s). arXiv:1502.04378

P.H.Tsang, in collaboration with H.M.Fried, Y.Gabellini, T. Grandou, Y.-M.Sheu, - A new approach to analytic, non-perturbative, gauge-invariant QCD renormalization is described, with applications to high energy elastic pp-scattering. Proceedings for the International Conference in New Frontiers of Physics, Crete, 2015. (submitted) arXiv:1511.08202

TALKS:

Sept 2004 - "Bacterial Adhesion by holdfast gel", 20th New England Complex Fluids Workshop

Dec 2014 - "Model of QCD Renormalization applied to pp scattering", - Joburg Workshop on Matrices, Holography and QCD.

February 2015 - "Model QCD Renormalization applied to pp scattering", 4th Winter Workshop on Non-Perturbative Quantum Field Theory.

August 2015 - "Exact, Finite, Model Renormalization of Non-Perturbative, Gauge-Invariant Realistic QCD", 4th International Conference on New Frontiers in Physics.

October 2015 - "From the smallest objects to the biggest puzzles: quarks and the solution to one of the 7 millenium problems.", Science Seminar (General Audience) - Bryant University.

November 2015 - "Analytic QCD - pp-scattering amplitudes", Seminar (short talk) - University of Connecticut.

SELECTED AWARDS:

National Science Scholar

Westinghouse Science Talent search - Semi Finalist

MIT class of 1935? fellowship

1st Place - Physics - Junior Engineering Technology and Science Contest (New York City)

Math fair Science fair - Gold/Silver medals.

WORK EXPERIENCE:

MIT - Whitehead Institute for Biomedical Research - Research student 1994-1995 (Prof. Paul Soloway and Prof. Rudolph Jaenisch)

Harvard Medical School/Mass. Eye and Ear Infirmary - Berman-Gund - Research Student (Prof. Tiansen Li and Prof. Eliot L. Berson) 1995-1996

Brown University - Teaching Assistant 1997-1998

Forbes.com - Software Engineer/Programmer. 1998 - 1999

Gobi Inc - Programmer 1999

Gobi Inc - Chief Technology Officer. 1999 - 2000

Advantage Realty of Forest Hills, Inc. NY. President/Real Estate Broker. 1997 - current

(The author took time off from school to run the family's business immediately after his father's passing in order to support the family. He now devotes full time to Physics.)

Bryant University - Adjunct Professor (Physics, Astronomy, Energy/Climate) 2006 - current

Acknowledgments

We thank Prof. Herbert M. Fried at Brown University, Prof. Yves Gabellini, Prof. Thierry Grandou, Dr. Yeuan-Ming Sheu(Brown University) at INLN, CNRS for their support and guidance. We also thank Prof. Ian Dell'Antonio, Prof. Chung-I Tan, Prof. Antal Jevicki, Prof. David Cutts, Dr. Walter Becker for their advice and guidance. This research was also made possible through the support of a Grant from the Julian Schwinger Foundation. The opinions expressed in this publication are those of the author and do not necessarily reflect the views of the Julian Schwinger Foundation. We especially wish to thank Mario Gattobigio for his many kind and informative conversations relevant to the Nuclear Physics aspects of our work.

Contents

List of Figures

List of Tables

Chapter 1

Introduction

1.1 Yang Mills and QCD

Yang-Mills theory, also known as "non-abelian gauge theory" [61] has an interesting history from the work of gauge symmetry that evolved from the work of Hermann Weyl [50].

Yang-Mills equations have common properties with Maxwell equations in that they provide classical description of massless waves. In the 1950's when Yang-Mills was discovered, it was already known that Quantum Electrodynamics gives extremely accurate experimental comparisons. However, the massless nature of classical Yang-Mills waves is an obstacle in applying Yang-Mills to nuclear forces, where forces are short ranged and particles are massive. In the case of the weak force, Glashow-Salam-Weinberg's electroweak theory used gauge group $H = SU(2) \times U(1)$. The massless nature of classical Yang-Mills waves were avoided with the addition of the Higgs field.

In the case of the strong force, the discovery of Asymptotic freedom, rather than the addition of fields to quantum Yang-Mills [37, 54]. Asymptotic freedom means that at short distances, fields display quantum behaviors similiar to its classical ones. At long distances, however, classical theory is not a good indicator for the quantum behaviors. Asymptotic freedom together with other experimental and theoretical results in the 1960's and 1970's made it possible to describe the strong force by a non-abelian gauge theory with gauge group $G = SU(3)$. The additional fields

describe quarks with spin $1/2$ that are perhaps analogous to the electron. Quarks, however transform under the representation of $SU(3)$. This non-abelian gauge theory of the strong force is called Quantum Chromodynamics (QCD).

For QCD to describe the strong force successfully, it must have at the quantum level the following three properties as described in one of the Millenium Problems by the Clay Mathematics Institute:

1) It must have a mass gap, $\Delta > 0$, such that every excitation of the vacuum has energy at least Δ. 2) It must have "quark confinement," that is, even though the theory is described in terms of elementary fields, such as quark fields, that transform non-trivially under $SU(3)$, the physical particle states – such as the proton, neutron, and pion –are $SU(3)$-invariant. 3) It must have "chiral symmetry breaking," which means that the vacuum is potentially invariant (in the limit that the quark-bare masses vanish) only under certain subgroup of the full symmetry group that acts on the quark fields.

The first point insures that strong forces are short ranged, the second point explains why quarks are never observed experimentally except in bound states, the third point is needed to account for the current algebra of soft pions.

Both experiment and computer simulations suggest strongly that QCD does have the three properties. QCD, however, are not fully understood theoretically. "There does not exist a convincing, whether or not mathematically complete, theoretical computation demonstrating any of the three properties in QCD, as opposed to a severly simplified truncation of it." [40] Despite many empirical successes in QCD, many fundamental questions remain unsolved. Questions include hadronization, color confinement, the behavior of QCD couping at small momenta, asymptotic $n!$ growth of the perturbation theory, also known as renormalon phenomena, the diffractive phenomena, a fundamental understanding of the soft and hard pomeron in high energy scattering, and the conflict between QCD vacuum structure and the small size of the cosmological constant [9].

1.2 Running Couplings

QCD running coupling can be obtained from integrating the differential equation

$$\mu^2 \frac{d\alpha_s}{d\mu^2} = \beta(\alpha_s) \tag{1.1}$$

rewritten as

$$\ln \frac{\mu^2}{\mu_0^2} = \int_{\alpha_s(\mu_0^2)}^{\alpha_s(\mu^2)} \frac{d\alpha}{\beta(\alpha)} \tag{1.2}$$

The resulting form is

$$\alpha_s(\mu^2) = \frac{1}{\beta_0 ln(\mu^2/\Lambda^2)} \tag{1.3}$$

The dimensional scale Λ keeps track of initial parametrization $(\mu_0, \alpha_s(\mu_0^2))$. The value of Λ must be extracted from experimental measurement of α_s for a given reference scale. This emergence of a scale parameter, referred to as dimensional transmutation, breaks the scale invariance of massless theories. This scale parameter is believed to be associated the hadron size. Λ is the scale about which the coupling (one-loop) diverges, the Landau ghost, and where pertubation theory becomes meaningless. This dimensional scale is scheme-dependent and receives further correction at each loop level [55].

1.3 Confinement and conformal algebraic structures'

In Brodsky and company's work, Light Front (LF) Hamiltonian theory provided a rigorous relativistic and frame independent framework for non-perturbative QCD and understanding color confinement. For QCD$(1+1)$, eigenstates for baryons and mesons at zero quark mass is determined in units of its dimensionful coupling with the Discretized Light Cone Quantization (DLCQ) [52, 51]. In the case of $3+1$ dimension, QCD's coupling is dimensionless, thus, it is not clear what sets the hadron mass. Instead, the work by de Alfaro, Fubini and Furlan (dAFF) can generate a mass scale and a confinement potential without changing the conformal invariance of the action. [48]. Thus, effective LF confining potential can be obtained by extending the

results found by dAFF to light-front dynamics and to the embedding space [11].

Brodsky and company and work in Charmonium showed that an effective harmonic potential in the light-front form of dynamics, for light quark masses, corresponds to a linear potential in the usual instant-form [60, 17]. These results give the prediction of linear Regge trajectories in the hadron mass square for small quark masses, in agreement with observations for light hadrons. 4 dimensional light-front dynamics combined with 5 dimensional AdS_5, with the extraction of mass scale from dAFF in $1+1$ dimension gives rise to $SO(2,1)$, an isometry group of AdS_2. Stated another way, the emergence of a mass scale comes from the remarkable connection between semiclassical light-front dyamics in four-dimension with gravity in higher dimensional AdS space, with constraints imposed by the dAFF one dimensional quantum field theory. [10].

1.4 Hadrons and Meson Spectrum

With LF Hamiltonian, hadronic states are arrived at in:

$$[-\frac{z^{d-1-2J}}{e^{\varphi(z)}}(\frac{e^{\varphi(z)}}{z^{d-1-2J}}\partial_z) + \frac{(mR)^2}{z^2}]\Phi_J(z) = M^2\Phi_J(z), \tag{1.4}$$

where invariant hadron mass $P_\mu P^\mu \equiv \eta^{\mu\nu}P_\mu P_\nu \equiv M^2$ The AdS mass $m = \mu_{eff} = \mu$ in the equation is a constant that is determined from the mapping of the light-front Hamiltonian. m maps to the Casimir operator of the orbital angular momentum in the light front. See Figure 1-2.

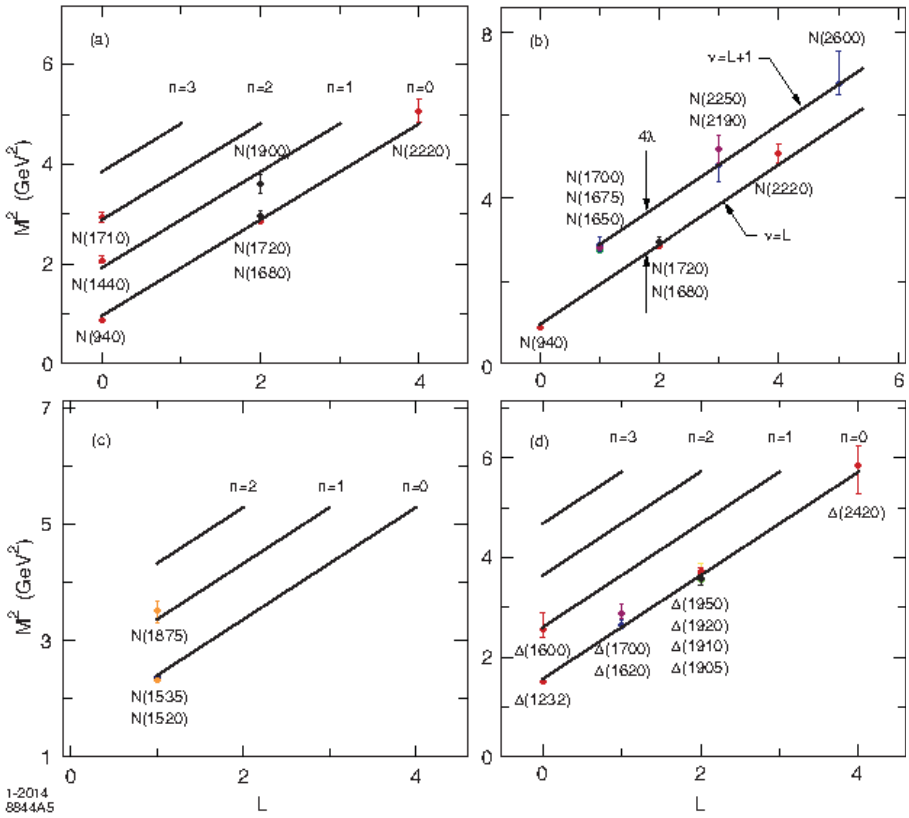

Figure 1-1: Meson spectrum [10]

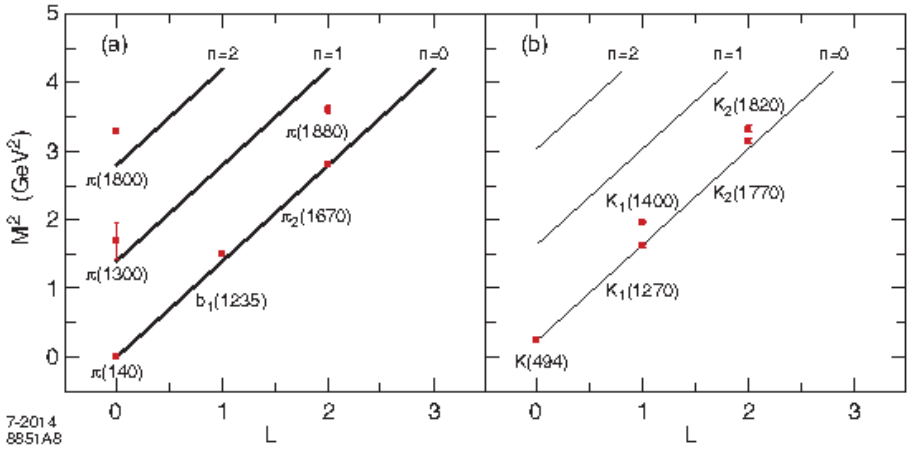

Figure 1-2: Meson spectrum [10]

Chapter 2

High Energy Scattering

The Balitsky-Fadin-Kuraev-Lipatov (BFKL) [44, 20, 43, 42, 5, 6] formalism enables the logarithms appearing in scattering amplitudes with large center of mass energy, $\sqrt{s}$ and fixed momentum transfer $\sqrt{-t}$ to be summed. Calculations of strong coupling high energy scattering at HERA, the Tevatron and LHC has used DGLAP and BFKL [56]. The Dokshitzer-Gribov-Lipatov-Alterelli-Parisi, DGLAP equation and the Balitsky-Fadin-Kuraev-Lipatov (BFKL) equation formed the basis for current understanding of high-energy scattering in quantum chromodynamics. See Figure [**?**].

Without an analytic QCD solution, calculations had to resort to studying unitarity and analyticity constraints on scattering amplitudes, combined with the work of Tullio Regge. Gribov, Lipatov and others developed the leading logarithm approximation to processes at high-energies. This is central to perturbative QCD for strong interactions. Reggeon field theory was checked and confirmed with QED experiments.

Experiments in the 1960s at SLAC had showed Bjorken scaling in deep inelastic lepton-hadron scattering. Gribov attemped to see if Bjorken scaling can be derived from QFT. For large momentum transfer, leading Feynman diagrams in QED gave rise to the logarithmically enhanced contributions to the cross section at fixed values of the Bjorken variable, $x = q^2/(s + q^2)$ between 0 and 1 [36].

Lipatov showed that the gauge vector boson in Yang-Mills theory is reggeized with radiative corrections included [45]. The vector boson becomes a moving pole in the complex angular momentum plane near $j = 1$. In QCD, this pole corresponds to color

exchange. The exchange of two or more reggeized gluons leads to colorless exchange in the t-channel. This exchange with vacuum quantum numbers is a Pomeron, and with non-vacuum ones is an Odderon.

Lipatov and collaborators showed that Pomeron correspond to a regge cut, and not a pole in the complex angular momentum plane.

2.1 BFKL and DGLAP

Quantum field theory is the heart of QCD, however, attempts towards solving QFT for strong interactions have been difficult. Some fifty years ago, efforts have been made to circumvent traditional QFT by focusing on unitarity and analyticity on scattering amplitudes, combined with extensions to Tullio Regge's work on connecting complex angular momentum to relativistic theory. Balitsky, Fadin, Kuraev and Lipatov (BFKL), over two decades ago, set out to determine the high-energy behavior of the scattering of hadronic objects within perturbative QCD. They found terms going as $(\alpha_s \ln s)^n$, where s is the squared centre-of-mass energy. Since the factor lns can compensate the smallness of $\bar{\alpha}_s$, it was necessary to sum the entire series of leading logarithmic, LL, terms. The resulting cross-section increases as a power of s^2. For typical values of $\alpha_s \approx 0.2$, this power is of the order of 0.5 [42, 5].

Much experimental effort has been devoted towards observing this phenomenon in the 1990's, however, experiments showed that the cross sections rise is much slower than $s = 0.5$.

The solution to this problem was to have been in determining the next-to-leading corrections to the BFKL equation, terms $\alpha_s(\alpha_s \ln s)^n$. After much effort, however, the next-to-leading order showed to be much smaller and the leading contribution, and, in fact, turned out not even positive definite [57].

Lipatov and collaborators showed that the Pomeron corresponds to a cut, and not a pole, in the complex angular momentum plane. Lipatov discovered beautiful symmetries in the BFKL equation. This enabled him to obtain solutions in terms of the conformal-symmetric eigenfunctions. This completed the construction of the

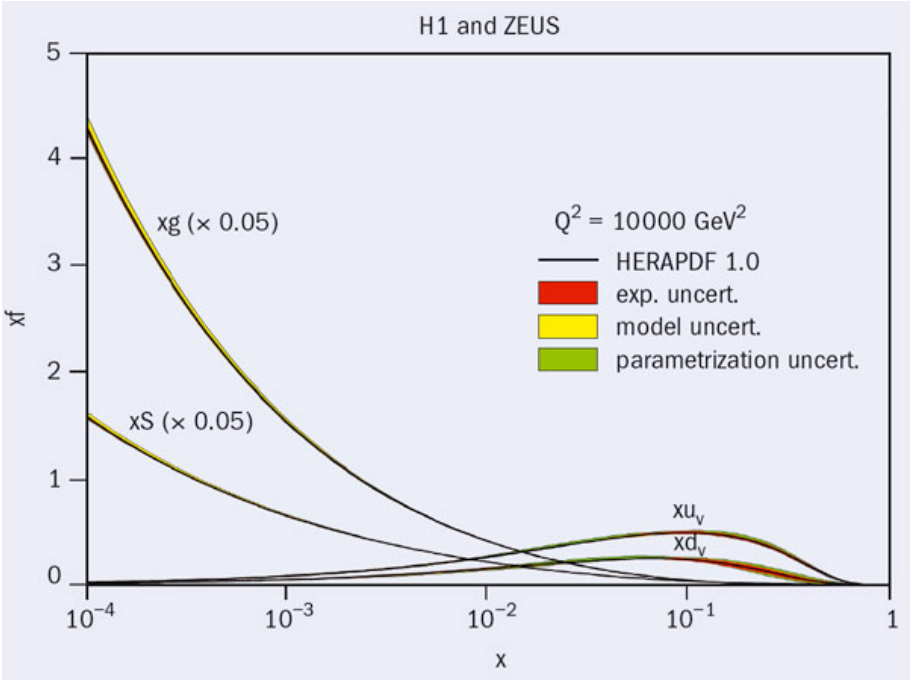

Figure 2-1: DGLAP equations allows the extraction of parton distribution functiosn from data at the electron-proton collider HERA. The proton-parton densities has been extracted from the combined H1 and ZEUS measurements in this figure, for $q^2 = 10,000 GeV^2$. This corresponds to W production at the LHC. xg is the gluon term that dominates the proton content at low Bjorken-x [41].

fundamental entity in high-energy physics in the bare Pomeron in QCD [46].

2.2 Donnachie and Landshoff

Regge theory has been hugely successful when compared with experimental data [16]. However there is significant gap in its understanding. Only exchanges of single particles can be calculated after five decades. Double or high exchanges has yet to be done. The accurate description of experimental data can only be achieved with the introduction of an exchange, the Pomeron, not obviously associated with particle exchange. According to Regge theory, particle exchange contributes simple power behavior s^{ϵ} to total cross sections. Donnachie and Landshoff, three decades ago, introduced just two powers to fit all hadron-hadron total cross sections. They showed with $\epsilon \approx 0.08$ corresponds to pomeron exchange and $\epsilon_R \approx \frac{1}{2}$ to nearly degenerate ρ, ω, f_2, a_2 exchange.

With deep inelastic ep scattering at small x from HERA, Donnachie and Landshoff introduced a second pomeron, the hard pomeron. This put the conventional DGLAP evolution analysis at small x in sound footing [16]. Without the second pomeron, unitarity would be violated as the forward amplitude would grow very large with increasing energy. Additional terms beyond P and PP would be ultimately necessary for higher energies to prevent the total cross section from becoming negative because the two pomeron PP term is negative, to preserve unitarity, but grows much more rapidly than P.

For the total cross section, $\sigma_{total} = Im\ A(s,0)$, Donnachie and Landshoff has

$$\begin{aligned} A(s,t) = &- \frac{X_P F_P(t)}{2\nu}\ e^{-\frac{1}{2}i\pi\alpha_P(t)}\ (2\nu\alpha'_P)^{\alpha_P(t)} - \frac{X_+ F_+(t)}{2\nu}\ e^{-\frac{1}{2}i\pi\alpha_+(t)}\ (2\nu\alpha'_+)^{\alpha_+(t)} \\ &\mp \frac{iX_- F_-(t)}{2\nu}\ e^{-\frac{1}{2}i\pi\alpha_-(t)}\ (2\nu\alpha'_-)^{\alpha_-(t)} \end{aligned} \tag{2.1}$$

where $\alpha_i(t) = 1 + \epsilon_i + \alpha'_i t \quad i = P, \pm$ and $F(t) = Ae^{at} + (1-A)e^{bt}$, see figure 2-2

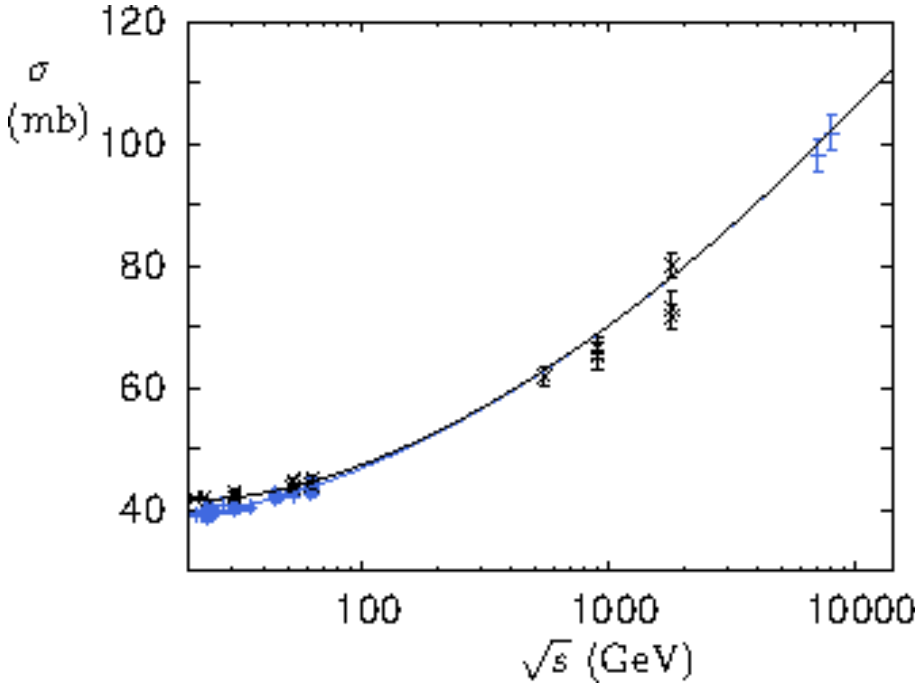

Figure 2-2: Total cross section with Reggeon and Pomeron [16]

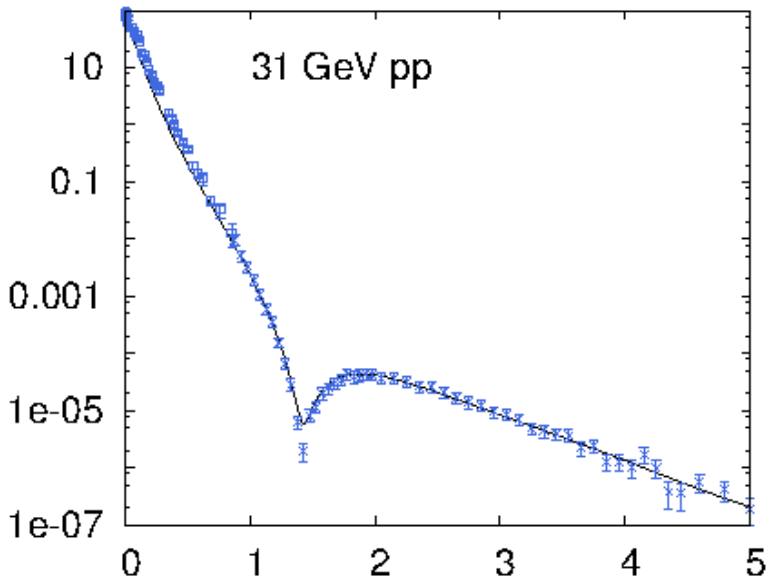

Figure 2-3: Differential cross section for elastic pp with Reggeon and Pomeron [16]

2.3 AdS/CFT - Tan and company.

In recent years, the AdS/CFT correspondence has been heavily investigated for QCD processes. Curved space string theory was first used to describe the classical Regge regime, where $s > \Lambda^2_{QCD}$ and the BFKL regime. A coherent treatment of the Pomeron based on AdS/CFT was presented by Brower, Polchinski, Strassler and Tan in 2006 [12]. String theory in flat space generally disagree with QCD, however, in the classic Regge regime, where $s \gg \Lambda^2_{QCD}$ and $|t| \leq \Lambda^2_{QCD}$, QCD scattering processes shows amplitudes similar to Regge behavior or that of flat-space classical string theory. For $s \gg -t \gg \Lambda_{QCD}$, string amplitudes follows a linear Regge trajectory while QCD does not. The asymptotic Regge regime is important because it accounts for most of total cross-sections and differential cross-sections at small angles, on the other hand however, direct perturbative computation nor lattice QCD methods can obtain QCD amplitudes. In string theory, the Pomeron is the object exchanged at tree level scattering in the Regime regime. That is, the graviton's Regge trajectory. Multi-Pomeron exchange becomes dominant as $s \to \infty$, and as such, non-perturbative approach to Pomerons is needed [13, 14].

Lipatov also considered the BFKL and DGLAP equations in N=4 theory and computed the anomalous dimensions of various operators. The high symmetry of N=4 SYM allowed calculations to be made to unprecedented high orders and the results were then compared with the predictions of string theory. This facilitated the study of integrable structures [47].

Lipatov established that the gluon production amplitudes in the planar approximation can have Mandelstam cut contributions in the multi-regge kinematics at some physical regions. The wavefunction of these states, in the adjoint representation, satisfy BFKL-like equation. They are integrable in leading logarithmic approximation and have the property of holomorphic factorization [47].

The resulting holomorphic hamiltonian coincides with an integrable open Heisenberg spin model's hamiltonian. A simple recurrent relation is obtained for the Baxter-Sklyanin equation for this model in terms of Γ-functions.

In 2007, Tan and company derived the Eikonal approximation for multiple Pomeron exchanges. Single Pomeron and multiple graviton exchange in AdS are generalized to consider unitarity and saturation in the conformal regime. This Eikonal indicates that the Froissart bound is satisfied and saturated [13, 14].

Alday and Maldacena in 2007 also wrote down gluon scattering amplitudes at strong coupling in $N = 4$ super Yang Mills using gauge/string duality [1]. Solutions were arrived at by finding classical string configurations with boundary conditions determined by gluon momenta. These solutions are infrared divergent. The gravity version of dimensional regularization was used to define finite quantities. These results are in agreement with similar work by Bern, Dixon and Smirnov [7].

2.4 Eikonal Derivation from Martin Perl Page 41-43

Starting with the relativistic wave equation

$$[\nabla^2 + k^2]\psi(r) = U(r)\psi(r) \tag{2.2}$$

Following derivation given by Glauber (2GL), where $U(r)$ is complex. With incident wave $\psi_{inc}(r)$, moving in direction $+z$, being written as

$$\psi_{inc}(r) = e^{ikz}\phi(r) \tag{2.3}$$

where $\phi(r) = 1$ at $z = -\infty$. Inserting $\psi_{inc}(r)$ into above gives

$$[2ik\frac{d}{dz} + \nabla^2]\phi(r) = U(r)\phi(r). \tag{2.4}$$

Assume the potential varies slowly with r that the second derivative can be neglected, or

$$|\nabla^2\phi(r)| \ll |2ik\frac{d\phi(r)}{dz}| \tag{2.5}$$

Then we obtain

$$2ik\frac{d\phi(r)}{dz} = U(r)\phi(r) \tag{2.6}$$

and

$$\phi(r) = exp[\frac{-i}{2k}\int_{-\infty}^{z} U(x,y,z')dz']. \tag{2.7}$$

Insert this expression for $\phi(r)$ into $\psi_{inc}(r)$ gives

$$\psi_{inc}(r) = e^{ikz}exp[-\frac{i}{2k}\int_{-\infty}^{z} U(x,y,z')dz']. \tag{2.8}$$

From $\psi(r) = \psi_{inc}(r) + \psi_{scat}(r)$, and $R = r - r'$ where

$$\psi_{scat}(r) = \frac{1}{4\pi}\int d^3r[U(r')\psi(r')\frac{e^{ikR}}{R}] \tag{2.9}$$

We obtain

$$\psi_{scat} = -\frac{1}{4\pi}\int d^3r[U(r)e^{ikz}exp(-\frac{i}{2k}\int_{-\infty}^{z} U(x,y,z')dz')\frac{e^{ikR}}{R}] \tag{2.10}$$

Remembering that $\psi_{scat}(r) = f(\theta)\frac{e^{ikr}}{r}$ with $f(\theta) = -\frac{1}{4\pi}\int d^3r[U(r')e^{i(k-k')\cdot r'}]$,
we arrive at the eikonal approximation

$$f(\theta) = -\frac{1}{4\pi}\int d^3r[e^{i(k-k')\cdot r}U(r)exp(-\frac{i}{2k}\int_{-\infty}^{z} U(x,y,z')dz')]. \tag{2.11}$$

For $b = z$, $(k-k')\cdot r = q\cdot r \approx q\cdot b$,
above becomes

$$f(\theta) = \frac{k}{2\pi i}\int d^2be^{iq\cdot b}exp[\frac{-i}{2k}\int_{-\infty}^{+\infty} U(b,z)dz] - 1 \tag{2.12}$$

If we define $\chi(b) = \chi_i(x,y,z=\infty)$, we get the common form of the eikonal model:

$$f(\theta) = \frac{k}{2\pi i}\int d^2be^{iq\cdot b}[e^{i\chi(b)} - 1] \tag{2.13}$$

see "High Energy Hadron Physics" by Martin L. Perl [53].

Chapter 3

Halpern Functional Integral

3.1 Field-Strength Formulation of Quantum Chromodynamics

In 1977, Halpern in an attempt to extend non-abelian gauge theories in space-time dimensions to $D \geq 3$ provided the follow work in this section. Non-abelian gauge theories is reformulated in terms of field strengths and the details for $(D = 4)$ QCD is written down [38, 39].

Starting with the action for QCD,

$$\begin{aligned} S_1 &= \int d^D x[\frac{1}{2}G^i_{\mu\nu}F^i_{\mu\nu} - \frac{1}{4}G^i_{\mu\nu}G^i_{\mu\nu} + \psi^\dagger(\not{\partial} + M + ig\ \not{V})\psi], \\ F^i_{\mu\nu} &\equiv \partial_\mu V^i_\nu - \partial_\nu V^i_\nu - gf^{ijk}V^j_\mu V^k_\nu, \\ \not{V} &\equiv \gamma_\mu V^a_\mu \frac{\lambda_a}{z} \end{aligned} \tag{3.1}$$

For the Generating Functional, we integrate e^{S_1} over all $G^i_{\mu\nu}$,V^i_μ,ψ,$\psi^\dagger$. After quadratic

integration over the V^i_μ, we obtain the field-strengh action,

$$\begin{aligned} S = \int d^D\chi [& \frac{1}{2g}(\partial_\rho G^i_{\mu\nu} - gJ^i_\mu)(\mathcal{G}^{-1})^{ij}_{\mu\nu}(\partial_\lambda G^j_{\lambda\nu} - gJ^j_\nu) \\ & - \frac{1}{4}G^i_{\mu\nu}G^i_{\mu\nu} + \psi^\dagger(\not{\partial} + M)\psi \\ & - \chi^i_{\mu\nu}\frac{g}{2}\mathcal{G}^{ij}_{\mu\nu}\chi^j_\nu], \\ J^i_\nu \equiv i\psi^\dagger\gamma_\mu\frac{\lambda^i}{2}\psi. & \end{aligned} \tag{3.2}$$

$\chi^i_{\mu\nu}$ is our familiar auxiliary field, much like a Faddeev-Popov field, representing $(det\mathcal{G})^{-1/2}$). In the case of $N = 2$, $D = 4$, we have

$$(\mathcal{G}^{-1})^{ij} = \tilde{G}^j G^i K^{-1} \tag{3.3}$$

where $K \equiv G^1\tilde{G}^2G^3 - G^3\tilde{G}^2G^1$ and $\tilde{G}^i_{\mu\nu} \equiv \frac{1}{2}\epsilon_{\mu\nu\rho\sigma}G^i_{\rho\sigma}$, $\epsilon_{0123} = +1$.

In the self dual sectors for K, $G^i = \pm\tilde{G}^i$,$G^i_{0l} \equiv E^i_l$, we obtain:

$$\begin{aligned} K_{\mu\nu} = \delta_{\mu\nu}\xi, \xi \equiv \frac{1}{3}\epsilon^{\alpha\beta\gamma}\epsilon_{ijk}E^\alpha_i E^\beta_j E^\gamma_k, \\ (\mathcal{G}^{-1})^{ij} = \pm\xi^{-1}G^jG^i. \end{aligned} \tag{3.4}$$

Under gauge transformations

$$\begin{aligned} V^i_\mu &\to O^{ia}V^a_\mu + \frac{1}{2g}f^{ijk}O^{ja}\partial_\mu(O^T)^{ak}, \\ G^k_{\mu\nu} &\to O^{kl}G^l_{\mu\nu}, \\ \mathcal{G}^{ij}_{\mu\nu} &\to O^{il}\mathcal{G}^{lm}_{\mu\nu}(O^T)^{mj}, \\ (\mathcal{G}^{-1})^{ij}_{\mu\nu} &\to O^{ib}(\mathcal{G}^{-1})^{ba}_{\mu\nu}(O^T)^{aj}) \end{aligned} \tag{3.5}$$

, the field equations are invariant. The action, however,

$$S = \int d^4\chi [\frac{1}{2g}(\partial G\ \mathcal{G}^{-1}\partial G) - \frac{1}{4}G^2 - \chi\frac{g}{2}\mathcal{G}\chi] \tag{3.6}$$

is not explicitly gauge-invariant.

To regain explicity gauge-invariance, we use identities,

$$\begin{aligned}\partial_\lambda G^i_{\mu\nu}(\mathcal{G}^{-1})^{ij}_{\mu\nu}\partial_\rho G^j_{\rho\nu} &= G^i_{\mu\nu}\epsilon^{ijk}\mathcal{J}^j_\mu\mathcal{J}^k_\nu \\ &= \partial_\lambda G^i_{\lambda\mu}\mathcal{J}^i_\mu \\ &= -G^i_{\lambda\mu}\partial_\lambda\mathcal{J}^i_\mu + \partial_\lambda(G^i_\lambda\mathcal{J}^i_\mu).\end{aligned} \tag{3.7}$$

With appropriate choices of the second and last term in Eq. 3.7 and dropping the surface term, we obtain explicit gauge-invariant form,

$$S = \int d^4\chi[-\frac{1}{2g}G\mathcal{F}(\mathcal{J}(G)) - \frac{1}{4}G^2 - \chi\frac{g}{2}\mathcal{G}\chi]. \tag{3.8}$$

Or

$$S = \int d^4\chi[-\frac{1}{4}(G + \frac{\mathcal{F}}{g})^2 + \frac{1}{8g^2}(\mathcal{F} \pm \tilde{\mathcal{F}})^2 \mp \frac{1}{4g^2}\mathcal{F}\tilde{\mathcal{F}}] \tag{3.9}$$

[38, 39]. At the saddle point, the first term in Eq. 3.8 vanishes and at fi xed $\int d^4\chi\mathcal{F}\tilde{\mathcal{F}}$, the action is minimum only if $\mathcal{F}\pm\tilde{\mathcal{F}} = 0$ and $G = \pm\tilde{\mathcal{G}}$. Rerranging Eq. 3.8 and Eq. 3.9 brings us to the form we shall use in our formalism,

$$S = \int d^4\chi[+\frac{1}{2g}G\chi + \chi^2]. \tag{3.10}$$

Chapter 4

Casimir Invariants

4.1 Casimir Invariants, C_2 and C_3

In non-relativistic Quark Models and in non-perturbative Schwinger mechanism, the dependence on the cubic Casimir operator, C_3 is important. In strong coupling fermionic QCD, the Green's functions and related amplitudes requires not just the $SU_c(3)$ quadratic Casimir operator, C_{2f} but also this C_3. C_3 accounts for the full algebraic content of the rank-2 Lie algebra of $SU_c(3)$ [29].

As pointed out by Grandou, it is remarkable that C_3 has been unnoticed for so long. Perhaps that is because numerically, C_3 only account for sub-leading effects [34].

4.2 Non-Perturbative Fermionic Green's Functions

In perturbation theory, all scattering processes are proportional to either $C_A = N_c$ and/or $C_F = (N_C^2 - 1)/2N_c$ [35]. In other words, processes are proportional to the quadratic Casimir operator eigenvalue $C_2(R)$ in the adjoint and fundamental representations. $C_2(R)$ is defined as:

$$C_2(R) = \sum_{a=1}^{8} T_a^2(R) \tag{4.1}$$

where $T_a(R)$ are the $SU_c(3)$ Lie algebra generators for a given representation R.

In addition to perturbative calculations, non-perturbative QCD models such as the MIT bag model, the Stochastic Vacuum Model (SVM), and Lattice QCD comply with these $C_2(R)$ dependencies.

In strong coupling where $g \gg 1$, the amplitude for Quark(antiQuark)/Quark(antiQuark) scattering amplitude using Random Matrix Theory is given by:

$$
\begin{aligned}
&(-16\pi\frac{m^2}{E^2})^N \sum_{\text{monomials}} (\pm 1)\,\mathrm{Tr} \prod_{1\le i\le N}^{\sum q_i = N(N-1)/2} [1 - i(-1)^{q_i}] \\
&\times C \int \mathrm{d}p_1 \,..\, \mathrm{d}p_{N(N-1)/2}\; f(p_1,\ldots,p_{N(N-1)/2}) \int_0^{+\infty} \mathrm{d}\alpha_1^i \;\frac{\sin[\alpha_1^i(\mathcal{O}\mathcal{T})_i]}{\alpha_1^i} \int_0^{+\infty} \mathrm{d}\alpha_2^i \;\frac{\sin[\alpha_2^i(\mathcal{O}\mathcal{T})_i]}{\alpha_2^i} \\
&\quad \times G_{34}^{23}\left(iN_c \left(\frac{\alpha_1^i\alpha_2^i}{g\varphi(b)}\right)^2 \frac{\hat{s}(\hat{s}-4m^2)}{2m^4} \,\middle|\, \begin{matrix} \frac{3-2q_i}{4}, & \frac{1}{2}, & 1, & \\ 1, & 1, & \frac{1}{2}, & \frac{1}{2} \end{matrix} \right),
\end{aligned}
\tag{4.2}
$$

where we have used the eikonal and quenced approximations, assumed single species of quarks of mass m.

$\mathcal{O} = \mathcal{O}(..,p_j,..)$ is an orthogonal $N \times N$ matrix specified by the $N(N-1)/2$ parmeters $p_j s$, with $N = D \times (N_c^2 - 1)$, D, the number of space-time dimensions; that is $N = 32$ [38, 39]. The distribution $f(..,p_j,..)$ defines the *Haar measure* of integration over the orthogonal group $O_N(\mathbb{R})$, and the constant C (the normalization) is the inverse of the $O_N(\mathbb{R})$-volume. $\mathcal{O}$, (the $N \times N$ orthogonal matrices), acts on N-vector of matrices $\mathcal{T} = (1,1,1,1) \otimes T = (T,T,T,T)$, i.e. $\mathcal{T}$ is made out of $D = 4$ copies of the full set T of $SU_c(3)$ generators, with the fundamental representation: $T = \{t_1, t_2, \ldots, t_7, t_8\}$, where $t_a = \lambda_a/2$ is the standard Gell-Mann matrices [62]. This step allows one to perform a series of exact integrations.

G_{34}^{23} is the Meijer special Functions [34].The Meijer function depends on an array of parameters, one of them involving an integer q_i, with $1 \le i \le N$ and $0 \le q_i \le N(N-1)/2$. The power of q_i comes from the expansion of a *Vandermonde determinant* into a sum of monomials.

Eq. 4.2 can now be rearranged to give,

$$\pm(-\frac{16\pi^2m^2}{E^2})^N \sum_{\text{monomials}} \Big\langle \prod_{i=1}^{N}[1-i(-1)^{q_i}] \times \left[\frac{\sqrt{2iN_c}\,\sqrt{\widehat{s}(\widehat{s}-4m^2)}}{m^2}\right]\frac{[(\mathcal{OT})_i]^{-2}}{g\varphi(b)} \times G_{03}^{30}\left(\left[\frac{g\varphi(b)}{\sqrt{32iN_c}}\frac{m^2}{\sqrt{\widehat{s}(\widehat{s}-4m^2)}}\right]^2\left[(\mathcal{OT})_i\right]^4\Big|\frac{1}{2},\frac{3+2q_i}{4},1\right)\Big\rangle_{O_N(\mathbb{R})}, \quad (4.3)$$

where the large brackets denote the orthogonal group $O_N(\mathbb{R})$. It is this group that displays the full algebraic content of rank-2 $SU_c(3)$ color algebra. The matrix values of the Meijer's function, G_{03}^{30} is,

$$z_i \equiv \lambda\,[(\mathcal{OT})_i]^4\,, \qquad \lambda \equiv \left(\frac{g\varphi(b)}{\sqrt{32iN_c}}\frac{m^2}{\sqrt{\widehat{s}(\widehat{s}-4m^2)}}\right)^2. \quad (4.4)$$

For $g \gg 1$ and $z_i \ll 1$ above can be rewritten as cite,

$$\pm(-\frac{4\pi^2m^2}{E^2})^N\Big\langle\prod_{i=1}^{N}[1-i(-1)^{q_i}]\sum_{h=1}^{3}A_i^h\,z_i^{\,b_h-\frac{1}{2}}\left(1+O_{ih}\,z_i+\mathcal{O}(z_i^2)\right)\Big\rangle_{O_N(\mathbb{R})}. \quad (4.5)$$

The matrix-valued argument z_i is on the order of $[(\mathcal{OT})_i]^4$. and tThe orders z_i^0, $\sqrt{z_i}$, z_i and $z_i\sqrt{z_i}$ contributions of (4.5), are of even orders $(\mathcal{OT})_i^0$, $(\mathcal{OT})_i^2$, $(\mathcal{OT})_i^4$ and $(\mathcal{OT})_i^6$ respectively.

The leading order $<\sqrt{z_i}>$ given by

$$\sqrt{\lambda}\sum_{j,k=1}^{N}\left\langle\mathcal{O}^{ij}\mathcal{T}_j\mathcal{O}^{ik}\mathcal{T}_k\right\rangle_{\varepsilon,\Theta} = \sqrt{\lambda}\left\langle\sum_{j=1}^{N}a_{ij}^2(\dots\Theta_{lm}\dots)\right\rangle_{\Theta}\mathcal{T}_j^2 = \frac{\sqrt{\lambda}}{N}\,DC_{2f}\,\mathbf{1}_{3\times3}\,, \quad (4.6)$$

where C_{2f} is the quadratic Casimir operator eigenvalue on the fundamental representation, $C_{2f} = C_F = 4/3$. $\mathbf{1}_{3\times3}$ is 3×3 identity matrix.

The sub-leading order is then,

$$< z_i >= (\frac{\sqrt{\lambda}}{N})^2\left((DC_{2f})^2 + (DC_{3f})\right)\mathbf{1}_{3\times3}\,, \quad (4.7)$$

where we see the cubic Casimir operator, C_{3f}, with fundamental representation,

$$\sum_{a,b,c=1}^{N_c^2-1} d_{abc}\, t^a t^b t^c \equiv C_{3f}\mathbf{1}_{3\times 3}\ . \tag{4.8}$$

In Young Tableaus parameters p, q, we have

$$C_3(p,q) = \frac{1}{18}(p-q)(2p+q+3)(2q+p+3). \tag{4.9}$$

Hence, in the $SU(3)$ fundamental representation,

$$C_{3f} = C_3(1,0) = \frac{10}{9}. \tag{4.10}$$

. And in the adjoint representation,

$$C_{3a} = C_3(1,1) = 0. \tag{4.11}$$

The next to sub-leading order $z_i\sqrt{z_i}$ is given by a combination of C_2's and C_3's,

$$< z_i\sqrt{z_i} > = (\frac{\sqrt{\lambda}}{N})^3 \left([2 + (\frac{5}{6})^2](DC_{2f})^2 + (DC_{2f})(DC_{3f}) + 3(DC_{3f}) \right) \mathbf{1}_{3\times 3}\,. \tag{4.12}$$

.

It is now clear that C_3 in addition to C_2 will be important in any non-perturbative fermionic Green's function and related processes [34, 35].

Chapter 5

Schwinger Action Principle and Generating Functional

5.1 Schwinger Action Principle

We begin by writing down the Schwinger's Action Principle [58] for the probability amplitude $< a, t_2|a', t_1 >$,

$$\delta < a, t_2|a', t_1 >= i < a, t_2|\delta W|a', t_1 > \tag{5.1}$$

where a denotes all appropriate set of eigenvalues, discrete or continuous, that characterize the system at time t. δW denotes variations in the parametric, end-point, and parameters which the Lagrangian itself may depend on. We assume the property of reality

$$< a, t_2|a', t_1 > \cdot =< a', t_1|a, t_2 > \tag{5.2}$$

and closure

$$\sum_n < a, t_2|n', t >< n', t|a', t_1 >=< a, t_2|a', t_1 > \tag{5.3}$$

The unitary operator U acting on a state vector $|a, t >$ corresponds to infinitesimal

transformation is

$$\begin{aligned} \delta|a,t> &= -iG(t)|a,t> \\ \delta<a,t| &= +i<a,t|G(t), \end{aligned} \tag{5.4}$$

where G is defined by the infinitesimal operator $\delta(U-1) = -iG$. Then combining Eq. 5.1 and Eq. 5.4 gives

$$\delta W = G(t_2) - G(t_1) \tag{5.5}$$

and with total variation $\delta Q = \delta_0 Q + \delta t \cdot dQ/dt$ giving $\delta W = Q \cdot P - \delta t \cdot H_{21}$ with $P = \partial L \partial(dQ/dt)$ and $H = [dQ/dt] \cdot \partial L/\partial(dQ/dt) - L$. The quanties P and H are coefficients of end-point coordinates or time-variations are precisely the usual definition of momentum and hamiltonian.

Under variations in δQ, we obtain

$$G(t) = P\delta Q - H\delta t \tag{5.6}$$

as the infinitesimal unitary operator for transformations appropriate to coordinate changes and to time translations. It is important to point out that the fundamental statement of quantum physics is a consequence of above derivations. To see this, we choose an arbitrary operator O and write $O' = U \cdot OU^\dagger$, where $U^\dagger$ is Hermitian adjoint of U. From Eq. 5.4, we see that variation δQ can be written as $\delta Q = i[O, G]$. If we choose, as an example, $O = Q$, the generator G is given by Eq. 5.6 is

$$G = P\ \delta Q. \tag{5.7}$$

To satisfy relation $\delta Q = i[P\delta Q, Q]$, we must adopt

$$[O, P] = i \tag{5.8}$$

where, adjusting for the correct units, $h/2\pi$, then the right hand side of the total

variation of W

$$\delta W = \int dt \cdot \delta Q_0 \cdot \left(\frac{\partial L}{\partial Q} - \frac{d}{dt}[\frac{\partial L}{\partial (dQ/dt)}] \right) + \left(\delta Q_0 \cdot [\frac{\partial L}{\partial (dQ/dt)}] + \delta t \cdot L \right)_{21} \tag{5.9}$$

multiplies Eq. 5.8. As the traditional Action Principle asserts that only terms that depends on the end-time quantities are non-zero, the first term on the RHS of Eq. 5.9 is zero. So, it is from Schwinger's Action Principle that we arrive at the fundamental state of quantum physics, with the expression of the uncertainty principle restricting possible measurements of δQ and δP in a system.

In the vacuum having source field j, the probability amplitude to find the system at a time t_2 with known vacuum state at t_1 is

$$< 0, t_2 | 0, t_1 >_j \tag{5.10}$$

This is the quantity central to all formal functional descriptions. The Action Principle, Eq. 5.1 gives an immediate answer for explicit form of j dependence.

$$\frac{\delta}{\delta j(x)} < 0, t_2 | 0, t_1 >_j = i < 0, t_2 | \frac{\delta}{\delta j(x)} W_{2,1} | 0, t_1 >_j \tag{5.11}$$

The coefficients of the implicit variations vanishes for the j dependence on operators $A(x)$ because of Euler equations. We then have

$$\frac{\delta}{\delta j(x)} < 0, t_2 | 0, t_1 >_j = < 0, t_2 | A(x) | 0, t_1 >_j \tag{5.12}$$

and n_{th} derivative is, with ordered bracket,

$$(\frac{1}{n})^n [\frac{\delta}{\delta j(x_1)}] ... [\frac{\delta}{\delta j(x_n)}] < 0, t_2 | 0, t_1 >_j = < 0, t_2 | (A(x_1) ... A(x_n))_+ | 0, t_1 >_j \tag{5.13}$$

To construct the coefficient of the n_{th} power of j in a Taylor expansion, we set $j = 0$ and obtain

$$< 0, t_2 | 0, t_1 >_j = < 0, t_2 | (exp[i \int d^4x j(x) A(x)])_+ | 0, t_1 > \tag{5.14}$$

We introduce the unitary operator $t^{21}[j] = (exp[i\int_{t_1}^{t_2} d^4x j(x)A(x)])_+$. By taking the limit $t_2 \to \infty$ and $t_1 \to \infty$, the vaccuum expectation value of Eq. 5.14 defines the Generating Functional, GF, $\mathcal{Z}[j]$, or

$$\mathcal{Z}[j] =< 0, t_2|0, t_1 >_j = lim_{t_1\to\infty, t_2\to\infty} < 0, t_2|(exp[i\int_{t_1}^{t_2} d^4x j(x)A(x)])_+|0, t_1 > . \tag{5.15}$$

A formal functional solution for Eq. 5.10, $< 0, t_2|0, t_1 >_j$ can be obtained by writing down the differential equation

$$\begin{aligned} -iK_x[\frac{\delta}{\delta j(x)}] < 0, t_2|0, t_1 >_j &= < 0, t_2|(j(x) - ng[A(x)]^{n-1})|0, t_1 >_j \\ &= \left(j(x) - ng(\frac{1}{i})^{n-1}[\frac{\delta}{\delta j(x)}]^{n-1}\right) < 0, t_2|0, t_1 >_j \end{aligned} \tag{5.16}$$

where Euler equation has been used again to result in only explicit $A(x)$ dependences for j. Setting $g = 0$, we have

$$K_x[\frac{\delta}{\delta j(x)}] < 0, t_2|0, t_1 >_j^{g=0} = ij(x) < 0, t_2|0, t_1 >_j^{g=0} \tag{5.17}$$

whose solution is

$$< 0, t_2|0, t_1 >_j^0 = exp[\frac{i}{2}\int d^4x \int d^4y j(x)\Delta_c(x - y; m^2)j(y)] \tag{5.18}$$

where the integration is over all spatial points with all t between t_1 and t_2.

If we return to the Action Principle, we can construct a solution to the full Eq. 5.17. Considering variations in the coupling $g \to g + dg$,

$$\frac{\delta}{\delta g} < 0, t_2|0, t_1 >_j = -i < 0, t_2|\int_{t_1}^{t_2} d^4x[A(x)]^n|0, t_1 >_j, \tag{5.19}$$

giving

$$\frac{\delta}{\delta g} < 0, t_2|0, t_1 >_j = -i\int_{t_1}^{t_2} d^4x[\frac{1}{i}\frac{\delta}{\delta j(x)}]^n < 0, t_2|0, t_1 >_j \tag{5.20}$$

with solution

$$< 0, t_2|0, t_1 >_j = exp\{ -ig \int_{t_1}^{t_2} d^4x \ [\frac{1}{i}\frac{\delta}{\delta j(x)}]^n \} < 0, t_2|0, t_1 >_j^0 \tag{5.21}$$

or

$$< 0, t_2|0, t_1 >_j = exp\{ i \int_{t_1}^{t_2} d^4x \ \mathcal{L}'\{\frac{1}{i}\frac{\delta}{\delta j(x)}\}^n \} < 0, t_2|0, t_1 >_j^0 \tag{5.22}$$

The generalized form is then the Generating Functional,

$$\mathcal{Z}^{(0)}[j] =< 0, \infty|0, -\infty >_{j_\mu}^{g=0} = exp[\frac{i}{2}\int j_\mu D_{c,\mu\nu} j_\nu], \tag{5.23}$$

where $D_{c,\mu\nu}(x-y) = \delta_{\mu\nu}\Delta_c(x-y,m)|_{m\to 0}$ is the free photon propagator in the Feynman gauge. The GF for free fermions is written with the addition of Grassmann sources, $\eta_\alpha, \bar{\eta_\beta}$.

$$\mathcal{Z}^{(0)}[\bar{\eta}, \eta] =< 0, \infty|0, -\infty >_{\nu,\bar{\nu}}^0 = exp[i\int \bar{\eta} S_c \eta] \tag{5.24}$$

As in Eq. 5.14, we get GF for free fermions as

$$\mathcal{Z}^{(0)}[\bar{\eta}, \eta] =< 0| \ (exp[\ i\int [\bar{\eta}\psi + \bar{\psi}\eta]])_+ |0 > \tag{5.25}$$

where Grassmann η_α, $\bar{\eta_\beta}$ anticommute with each other and with all free fermion fields $\psi_\alpha^{(0)}$,$\bar{\psi}_\beta^{(0)}$.

The full GF with j, η and $\bar{\eta}$ is then, from Eq. 5.22, Eq. 5.24 and Eq. 5.25,

$$\begin{aligned}\mathcal{Z}[j, \bar{\eta}, \eta] &= \frac{1}{< 0, +\infty|0, \infty > |_{j=\bar{\eta}=\eta=0}} \cdot exp[-i\int \frac{\delta}{\delta\eta}(-g\gamma\cdot\frac{\delta}{\delta j})\frac{\delta}{\delta\bar{\eta}}] \cdot \mathcal{Z}^{(0)}[j] \cdot \mathcal{Z}^{(0)}[\bar{\eta}, \eta], \\ &= exp[-i\int \frac{\delta}{\delta\eta}(-g\gamma\cdot\frac{\delta}{\delta j})\frac{\delta}{\delta\bar{\eta}}] \cdot exp[\frac{i}{2}\int j_\mu D_{c,\mu\nu} j_\nu] \cdot exp[\ i\int [\bar{\eta}\psi + \bar{\psi}\eta]].\end{aligned} \tag{5.26}$$

The QCD Lagrangian is

$$\mathcal{L}_{QCD} = \frac{1}{4}\mathbf{F}_{\mu\nu}^a \mathbf{F}_{\mu\nu}^a - \bar{\psi}\cdot[m + \gamma_\mu(\partial_\mu - igA_\mu^a\lambda^a)]\cdot\psi, \tag{5.27}$$

where $\mathbf{F}^a_{\mu\nu} = \partial_\mu A^a_\nu - \partial_\nu A^a_\mu + g f^{abc} A^b_\mu A^c_\nu \equiv \mathbf{f}^a_{\mu\nu} + g f^{abc} A^b_\mu A^c_\nu$.

Rearranging the Lagrangian [26, 29, 25, 31], we use,

$$\begin{aligned} -\frac{1}{4}\int F^2 = -\frac{1}{4}\int f^2 - \frac{1}{4}\int [F^2 - f^2] = -\frac{1}{4}\int f^2 + \int \mathcal{L}'[A] \\ \mathbf{f}^{\ a}_{\mu\nu} = \partial_\mu A^a_\nu - \partial_\nu A^a_\mu \\ \mathcal{L}'[A] = -\frac{1}{4}(2\mathbf{f}^a_{\mu\nu} + g f^{abc} A^b_\mu A^c_\nu)(g f^{abc} A^b_\mu A^c_\nu) \end{aligned} \tag{5.28}$$

After integration by parts, we obtain

$$-\frac{1}{4}\int \mathbf{F}^2 = -\frac{1}{2}\int A^a_\mu(-\partial^2)A^a_\mu + \frac{1}{2}\int (\partial_\mu A^a_\mu)^2 + \int \mathcal{L}'[A] \tag{5.29}$$

To select a particular relativistic gauge, we multiply the term $\frac{1}{2}\int(\partial_\mu A^a_\mu)^2$ in Eq. 5.29 by λ. We include this term as part of the interaction and obtain

$$\mathcal{Z}^{(\zeta)}_{QCD}[j] = \mathcal{N} exp[i\int \mathcal{L}'[\frac{1}{i}\frac{\delta}{\delta j}]] \cdot exp[\frac{i}{2}\lambda \int \frac{\delta}{\delta j_\mu}\partial_\mu \partial_\nu \frac{\delta}{\delta j_\nu}] \cdot exp[\frac{i}{2}\int j \cdot D^{(0)}_c \cdot j], \tag{5.30}$$

or

$$\mathcal{Z}^{(\zeta)}[j] = \mathcal{N} exp[i\int \mathcal{L}'[\frac{1}{i}\frac{\delta}{\delta j}]] \cdot exp[\frac{i}{2}\int j \cdot D^{(\zeta)}_c \cdot j]. \tag{5.31}$$

Here, we have neglected the fermion/quark variables and will reinsert at the end. Replacing $\mathcal{L}'$ from Eq. 5.22 gives us,

$$\begin{aligned} \mathcal{Z}^{(\zeta)}_{QCD}[j] = \mathcal{N} exp[-\frac{i}{4}\int F^2 - \frac{i}{2}(1-\lambda)\int (\partial_\mu A^a_\mu)^2 + \frac{i}{2}\int A^a_\mu(-\partial^2)A^a_\mu]|_{A\to\frac{1}{i}\frac{\delta}{\delta j}} \\ \cdot exp[\frac{i}{2}\int j \cdot D^{(0)}_c \cdot j]. \end{aligned} \tag{5.32}$$

The choice of $\lambda = 1$ can now be made. An important consequence is that the term $exp[\frac{i}{2}\int A^a_\mu(-\partial^2)A^a_\mu]|_{A\to\frac{1}{i}\frac{\delta}{\delta j}}$ effectively removes all factors of $exp[\frac{i}{2}\int j\cdot D^{(0)}_c \cdot j]$, thereby gluons are treated, effectively as ghost fields and gluons themselves are never measurable by themselves. The result is the QCD Generating Functional, after reinserting

the fermion/quark variables,

$$\mathcal{Z}_{QCD}[j,\bar{\eta},\eta] = \mathcal{N} e^{-\frac{i}{2}\int \frac{\delta}{\delta A}\cdot D_A^{(0)}\cdot\frac{\delta}{\delta A}} \cdot e^{-\frac{i}{4}\int \mathbf{F}^2 + \frac{i}{2}\int A\cdot(-\partial^2)\cdot A} \cdot e^{i\int \bar{\eta}\cdot G_c[A]\cdot\eta + L[A]}\Big|_{A=\int D_c^{(0)}\cdot j} \tag{5.33}$$

The quark variables, $G[A]$ and $L[A]$ represents the quark line and quark loop respectively [21, 22]. We shall examine them more closely in next section.

5.2 Schwinger Generating Functional

From last section, we started with the Schwinger Generating Functional, GF, for QCD, with gluon operators in an Arbitrary, relativistic, gauge. The GF is rearranged in terms of a "Reciprocity Relation" under a "Gaussian Linkage Operation", $exp[-\frac{i}{2}\int \frac{\delta}{\delta A}\cdot D_A^{(0)}]$. The GF now depends upon two functionals of A,

$$\mathcal{Z}_{QCD}[j,\bar{\eta},\eta] = \mathcal{N} e^{-\frac{1}{2}\int \frac{\delta}{\delta A}\cdot D_c^{(0)}\cdot\frac{\delta}{\delta A}} \cdot e^{-\frac{i}{4}\int \mathbf{F}^2 + \frac{i}{2}\int A\cdot(-\partial^2)\cdot A} \cdot e^{i\int \bar{\eta}\cdot \mathbf{G}_c[A]\cdot\eta + \mathbf{L}[A]}\Big|_{A=\int \mathbf{D}_c^{(0)}\cdot j} \tag{5.34}$$

where the quark line, $\mathbf{G}_c[x,y|\mathbf{A}] = [m + \gamma\cdot(\delta - igA\tau)]^{-1}$ and virtual quark loop, $\mathbf{L}[\mathbf{A}] = \ln[1 - i\gamma\mathbf{A}\tau_c[0]]$.

The GF can now can be rearranged into gauge-invariant form. This was overlooked for decades [26, 24].

Now combine with Fradkin expressions for the quark line, $\mathbf{G}_c[A]$, and quark loop, $\mathbf{L}[A]$. Efimov S. Fradkin gave expressions for $\mathbf{G}_c[A]$ and $\mathbf{L}[A]$ in gaussian form [21, 22]. These are exact.

Fradkin's representation for the quark line, $\mathbf{G}[A]$ is given by

$$
\begin{aligned}
&\mathbf{G}_{\rm c}(x,y|A) \qquad\qquad (5.35)\\
= \;& i\int_0^\infty ds\; e^{-ism^2}\, e^{-\frac{1}{2}Tr\ln(2h)} \int d[u]\, e^{\frac{i}{4}\int_0^s ds'\,[u'(s')]^2}\,\delta^{(4)}(x-y+u(s))\\
&\times\left[m-\gamma_\mu\frac{\delta}{\delta u'_\mu(s)}\right]\mathcal{N}_\Omega\,\mathcal{N}_\Phi\int d[\alpha]\int d[\mathbf{\Xi}]\int d[\Omega]\int d[\mathbf{\Phi}]\,\left(e^{i\int_0^s ds'\left[\alpha^a(s')-i\sigma_{\mu\nu}\,\mathbf{\Xi}^a_{\mu\nu}(s')\right]\tau^a}\right)_+\\
&\times e^{-i\int ds'\,\Omega^a(s')\,\alpha^a(s')-i\int ds'\,\mathbf{\Phi}^a_{\mu\nu}(s')\,\mathbf{\Xi}^a_{\mu\nu}(s')}\\
&\times e^{-ig\int ds'\,u'_\mu(s')\,\Omega^a(s')\,A^a_\mu(y-u(s'))+ig\int ds'\,\mathbf{\Phi}^a_{\mu\nu}(s')\,\mathbf{F}^a_{\mu\nu}(y-u(s'))},
\end{aligned}
$$

while the Fradkin's representation for the quark loop, $\mathbf{L}[A]$ is given by

$$
\begin{aligned}
\mathbf{L}[A] \;=\; & -\frac{1}{2}\int_0^\infty\frac{ds}{s}\,e^{-ism^2}\,e^{-\frac{1}{2}Tr\ln(2h)} \qquad\qquad (5.36)\\
&\times\mathcal{N}_\Omega\,\mathcal{N}_\Phi\int d^4x\int \mathrm{d}[\alpha]\int \mathrm{d}[\Omega]\int \mathrm{d}[\mathbf{\Xi}]\int \mathrm{d}[\mathbf{\Phi}]\\
&\times\int d[v]\,\delta^{(4)}(v(s))\,e^{\frac{i}{4}\int_0^s ds'\,[v'(s')]^2}\\
&\times\; e^{-i\int ds'\,\Omega^a(s')\,\alpha^a(s')-i\int ds'\,\mathbf{\Phi}^a_{\mu\nu}(s')\,\mathbf{\Xi}^a_{\mu\nu}(s')}\cdot Tr\left(e^{i\int_0^s ds'\left[\alpha^a(s')-i\sigma_{\mu\nu}\,\mathbf{\Xi}^a_{\mu\nu}(s')\right]\tau^a}\right)_+\\
&\times e^{-ig\int_0^s ds'\,v'_\mu(s')\,\Omega^a(s')\,A^a_\mu(x-v(s'))-2ig\int d^4z\left(\partial_\nu\mathbf{\Phi}^a_{\nu\mu}(z)\right)A^a_\mu(z)}\\
&\times e^{+ig^2\int ds'\,f^{abc}\mathbf{\Phi}^a_{\mu\nu}(s')\,A^b_\mu(x-v(s'))\,A^c_\nu(x-v(s'))}\\
&-\{g=0\},
\end{aligned}
$$

See Appendix A for details on Fradkin's variables. The $\mathbf{F}^2$ in the GF Eq. 5.34 can be rewritten using Halpern's half century old expression [38, 39],

$$
e^{-\frac{i}{4}\int\mathbf{F}^2}=N\int d[\chi]e^{\frac{i}{4}\int\chi^2+\frac{i}{2}\int F\cdot\chi}, \qquad (5.37)
$$

where $\chi^a_{\mu\nu}=-\chi^a_{\nu\mu}$. With the $exp[-\frac{i}{4}\int\mathbf{F}^2]$ in the GF in Gaussian form, under χ fields, the relevant Gaussian Functional operations can be performed exactly. This corresponds to the summation of all Feynman graphs of gluons exchanged between quarks.

Then the explicit cancellation of all the gauge-dependent gluon propagators is

obtained as will be shown in next Chapter, Section 6.1.

5.3 The importance of non-perturbative solutions in QCD

Amongst the reasons that give perturbative QCD difficulties is because there are ,in effect, two coupling constants, Quarks and gluons, g_1 and g_2 respectively. Expansion around $g_2 = 0$ will not be sensible when we are looking at $\frac{g_1^2}{g_2}$ terms.

Chapter 6

Explicit Gauge Invariance

6.1 Gauge Cancellations

A rearrangement can now be made to formally insure gauge-invariance, even though the GF still apparently contains gauge-dependent gluon propagators.

$$\mathcal{Z}_{QCD}[j,\bar{\eta},\eta] = \mathcal{N} e^{-\frac{1}{2}\int \frac{\delta}{\delta A}\cdot D_c^{(0)}\cdot\frac{\delta}{\delta A}} \cdot e^{-\frac{i}{4}\int \mathbf{F}^2 + \frac{i}{2}\int A\cdot(-\partial^2)\cdot A} \cdot e^{i\int \bar{\eta}\cdot\mathbf{G}_c[A]\cdot\eta + \mathbf{L}[A]}\big|_{A=\int \mathbf{D}_c^{(0)}\cdot j} \tag{6.1}$$

Gives 2n-point functions:

$$= \mathcal{N}\int d[\chi] e^{\frac{i}{4}\int \chi^2} e^{\mathfrak{D}_A^{(0)}} e^{\frac{i}{2}\int \chi\cdot\mathbf{F} + \frac{i}{2}\int A\cdot(D_c^{(0)})^{-1}\cdot A} G_c(1|gA)G_c(2|gA)e^{L[A]}\big|_{A=0} \tag{6.2}$$

Then,

$$\begin{aligned} e^{\mathfrak{D}_a} F_1[A] = exp[\frac{i}{2}\int \bar{Q}\cdot D_c^{(0)}\cdot(1-\bar{K}\cdot D_c^{(0)})^{-1}\cdot\bar{Q} - \frac{1}{2}\mathrm{Tr}\ln(1-D_c\cdot\tilde{K})] \\ \cdot\ exp[\frac{1}{2}\int A\cdot\bar{K}\cdot(1-D_c^{(0)}\cdot\bar{K})^{-1}\cdot A + i\int \bar{Q}\cdot(q-\bar{K}\cdot D_c^{(0)})^{-1}] \end{aligned} \tag{6.3}$$

where

$$\begin{aligned} D_c^{(0)}\cdot(1-\bar{K}\cdot D_c^{(0)})^{-1} &= D_c^{(0)}\cdot[1-(\hat{K}+(D_c^{(0)})^{-1})\cdot D_c^{(0)}]^{-1} \\ &= -(\tilde{K}_{\mu\nu}^{ab} + g f^{abc}\chi_{\mu\nu}^c)^{-1} \\ &= -\hat{\mathbf{K}}^{-1} \end{aligned} \tag{6.4}$$

connects two quarks, forming the basis of our Gluon Bundle.

Remembering that $exp[\frac{i}{2}\int \frac{\delta}{\delta A'}\cdot D_c^{(0)}\cdot\frac{\delta}{\delta A'}]$ is the inverse of $e^{\mathfrak{D}_A}$, we arrive at

$$\begin{aligned} e^{\mathfrak{D}_A}F_1[A]F_2[A] = exp[-\frac{i}{2}\int \bar{Q}\cdot\hat{\mathbf{K}}^{-1}\cdot\bar{Q} + \frac{1}{2}\mathrm{Tr}\ln\hat{\mathbf{K}} + \frac{1}{2}\mathrm{Tr}\ln(-D_c^{(0)})] \\ \cdot\ exp[\frac{i}{2}\int \frac{\delta}{\delta A'}\cdot\mathbf{D}_c^{(0)}\cdot\frac{\delta}{\delta A'}] \\ \cdot exp[\frac{i}{2}\int \frac{\delta}{\delta A'}\cdot\hat{\mathbf{K}}^{-1}\cdot\frac{\delta}{\delta A'} - \int\bar{Q}\cdot\hat{\mathbf{K}}^{-1}\cdot\frac{\delta}{\delta A'}] \\ \cdot\ (e^{\mathfrak{D}_A}F_2[A']) \end{aligned} \tag{6.5}$$

$$\begin{aligned} e^{\mathfrak{D}_A}F_1[A]F_2[A] = \mathfrak{N}\ exp[-\frac{i}{2}\int \bar{Q}\cdot\hat{\mathbf{K}}^{-1}\cdot\bar{Q} + \frac{1}{2}\mathrm{Tr}\ln\hat{\mathbf{K}}] \\ \cdot exp[\frac{i}{2}\int \frac{\delta}{\delta A}\cdot\hat{\mathbf{K}}^{-1}\cdot\frac{\delta}{\delta A} - \int\bar{Q}\cdot\hat{\mathbf{K}}^{-1}\cdot\frac{\delta}{\delta A}] \\ \cdot exp[L[A]] \end{aligned} \tag{6.6}$$

As one sees in equation 6.6, all the explicit gauge dependent propagators cancel. This is gauge invariant by means of gauge-independence. It deserves to be emphasized that Gauge Independence is the strongest form of Gauge Invariance. Feynman had long hoped for this for QED.

The $-\hat{\mathbf{K}}^{-1}$ above, also written as $(f\cdot\chi)^{-1}$ represents infinite gluon exchanges summed. This term is the *Gluon Bundle*, GB, exchanged between two quarks as shown in figure 6-1.

Figure 6-1: A *Gluon Bundle*, GB, is the term $(f\cdot\chi)^{-1}$, representing the exchange of all gluons summed.

All the gaussian linkage operations can then be carried through exactly, corresponding to the summation of all gluons changed between any pair of quark (and/or anti-quark) lines, and including the cubic and quartic gluon interactions. See figure 6-2.

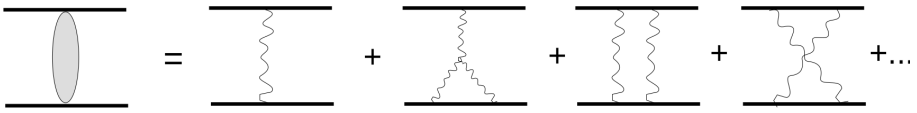

Figure 6-2: A *Gluon Bundle, GB, representing the exchange of all gluons summed.*

The result is explicit cancellation of all gauge-dependent gluon propagators, with resulting GF exhibiting Manifest Gauge Independence. One also finds a new, exact property of non-perturbative, gauge-invariant QCD, where the space-time coordinates of both ends of a GF are equal, modulo small uncertainties in their transverse coordinates. There is an Effective Locality between interacting quarks, and, changes all the remaining functional integrals into sets of ordinary integrals. One can actually complete these integrals [25, 26, 31]

Chapter 7

Effective Locality

7.1 Proof of Effective Locality for all quark processes.

Effective Locality is a new property where the coordinates between opposite end points of a Gluon Bundle was the same, modulo transverse quark fluctuations. This property holds true for all quark processes, without approximation and without exception. We prove this below.

In the QCD Generating Functional, we have used

$$e^{-\frac{i}{4}\int F^a_{\mu\nu}F^{\mu\nu}_a} = \mathfrak{N}\int d[\chi]e^{\frac{i}{4}\int \chi^a_{\mu\nu}\chi^{\mu\nu}_a + \frac{i}{2}\int \chi^a_{\mu\nu}F^{\mu\nu}_a} \tag{7.1}$$

and

$$\int d[\chi] = \prod_i \prod_a \prod_{\mu>\nu} \int d\chi^a_{\mu\nu}(\omega_i) \tag{7.2}$$

Each χ is divided into d^4 volume that is, not part of a function space but becomes individual minkowski space units[29].

$$p_1 + p_2 = p_1' + {}_2' \tag{7.3}$$

are obtained by pair-wise functional differentiation of the Generating Functional with respect to quark sources η^a_μ, $\bar{\eta}^b_\nu$. Each of these operations bring down a set of Green's

function, $G_c[A]$.

$$\mathfrak{N}\int d[\chi]e^{\frac{i}{4}\int\chi^2 e^{\mathfrak{D}_A}}e^{\frac{i}{2}\int\chi\mathbf{F}+\frac{\mathbf{i}}{\mathbf{2}}\int\mathbf{A}(\mathbf{D_c^\zeta})^{-\mathbf{1}}\mathbf{A}}\times[G_c^I(x_1,y_1|A)G_C^{II}(x_2,y_2|A)\frac{e^{L[A]}}{<S>}]_{A=0} \quad (7.4)$$

In the ordered exponentials definite the $G_c^{I,II}[A]$, linear A_μ dependencies can be factored out in:

$$(e^{g\int_0^s ds'\sigma\cdot F(y-u(s')}\cdot e^{-ig\int_0^s ds'u'(s')\cdot A(y-u(s'))})_+ \quad (7.5)$$

and

$$(exp[g\int_0^s ds'\sigma_{\mu\nu}\lambda^a f^{abc}A_\mu^b(z)A_\nu^c(z)])_+ \quad (7.6)$$

where $z=y-u(s')$.

For example,

$$(e^{2ig\int_{-\infty}^{+\infty}dsp_\mu A_\mu^a(y+2p)\lambda^a})_+=\int\mathfrak{D}\alpha\delta[\alpha^a(s)-2gp_\mu A_\mu^a(y+2sp)](e^{i\int_{-\infty}^{+\infty}ds\alpha^a(s)\lambda^a})_+ \quad (7.7)$$

The result is then

$$e^{-\frac{i}{2}\int\frac{\delta}{\delta A}\cdot D_c^{(\zeta)}\cdot\frac{\delta}{\delta A}}\cdot e^{+\frac{i}{2}\int A\cdot\bar{K}\cdot A+i\int\bar{Q}\cdot A}\cdot e^{L[A]} \quad (7.8)$$

where

$$\bar{K}_{\mu\nu}^{ab}=K_{\mu\nu}^{ab}+[gf^{abc}\chi_{\mu\nu}^c+(D_c^{(\zeta)})^{-1})_{\mu\nu}^{ab}] \quad (7.9)$$

and

$$\bar{Q}_\mu^a=-\partial_\nu\chi_{\mu\nu}^a+Q_\mu^a=-\partial_\nu\chi_{\mu\nu}^a+g[R_{I\mu}^a+R_{II\mu}^a] \quad (7.10)$$

The functional identity

$$e^{\mathfrak{D}_A} \cdot (F_I[A]F_{II}[A]) = (e^{\overleftrightarrow{\mathfrak{D}}_A} \cdot F_I[A]) \cdot e^D \cdot (e^{\mathfrak{D}_{A'}} \cdot F_{II}[A'])_{A'=A} \tag{7.11}$$

is required with the cross-linkage operator

$$\overleftrightarrow{\mathfrak{D}} = -i \int \frac{\overleftarrow{\delta}}{\delta A} \cdot D_c^{(\zeta)} \cdot \frac{\overrightarrow{\delta}}{\delta A'}, \tag{7.12}$$

.

As before, all correlation functions does not have D_c^ζ dependence, whereas $\hat{K} = K + g(f \cdot \chi)$ connects all quark lines and quark loops. Further, this connection by K is "effectively local" from

$$< x|\hat{K}^{-1}|y >= \hat{K}^{-1}(x)\delta^{(4)}(x-y) \tag{7.13}$$

.

A Gluon Bundle reduces coordinates at each end to depend only on the simple combination of y and Fradkin's variables $u(s')$ in a specific, for example, $y - u(s')$, local way.

Gluon propagators $D_c(w-z)$ in QCD quark/(anti)quark amplitudes are replaced by contact type interaction term $\hat{K}^{-1}(w) \times \delta^{(4)}(w-z)$.

For example, in the Bloch-Nordsieck approximation where

$$\begin{aligned} < p|G_c^{BN}[A]|y > = e^{-ip\cdot y} \cdot i \int_0^\infty ds e^{-is(m^2+p^2)} m - i\gamma_\mu [p_\mu - gA_\mu^a(+2sp)\lambda^a] \\ \times (exp\{g\int_0^s ds'\sigma^{\mu\nu}F_{\mu\nu}^a(y+2s'p)\lambda^a\} \cdot exp\{+2ig\int_0^s ds'[p^\mu A_\mu^a(y+2s'p)\lambda^a]\})_+ \end{aligned} \tag{7.14}$$

leads to

$$\delta^{(4)}(\omega - y_1 + s_1 p_1) \cdot \delta^{(4)}(\omega - y_2 + s_2 p_2)$$
$$= \frac{1}{2pE} \cdot \delta^{(2)}(\vec{y}_{1,\perp} - \vec{y}_{2,\perp}) \cdot \delta(s_1 - s_+) \cdot \delta(s_2 - s_-)$$
$$\cdot \delta^{(2)}(\vec{\omega}_\perp - \vec{y}_\perp \cdot \delta(\omega_L - \frac{1}{2}(y_{1,L} + y_{2,L})) \cdot \delta(\omega_0 - y_{1,0} + \frac{E}{p} y_{1,L}). \tag{7.15}$$

In the center of mass,

$$\vec{y}_\perp = \vec{y}_{1,\perp} = -\vec{y}_{2,\perp} \equiv \frac{1}{2}\vec{b},$$
$$z_0 = y_{1,0} - y_{2,0} = 0 \rightarrow s_1 = s_2 \tag{7.16}$$
$$y_{1,0} = \gamma m s_1 \rightarrow s_1 = \frac{y_{1,0}}{(\gamma m)}.$$

For large γ and any reasonable duration of the scattering, $s_1 = s_2 \approx 0$.

$$ig\delta^{(2)}(\vec{b})\Omega_I^a(0)[f \cdot \chi(\omega^{(0)}]^{-1}|_{3,0}^{ab}\Omega_{II}^b(0), \tag{7.17}$$

where $\omega_\mu^{(0)} = (\vec{y}_\perp, \vec{0}_L; y_0)$ for $E/p \approx 1$.

These statements all refer to particles. The longitudinal momenta of quarks can be obtained but the transverse coordinates cannot as required by the introduction of transverse quark imprecision $\varphi(b)$.

We now replace $\delta^{(2)}(\vec{y}_{1,\perp} - \vec{y}_{2,\perp} = \delta^{(2)}(\vec{b})$ by

$$(2\pi)^2 \int d^2\vec{k}_\perp e^{i\vec{k}_\perp \cdot \vec{b} - \vec{k}_\perp^2/M^2} = \frac{M^2}{4\pi} exp[-\frac{M^2\vec{b}^2}{4}] \tag{7.18}$$

where $M \approx$ (total center of mass scattering energy).

$$s_1 = s_2 = s \approx 0$$
$$\omega_\mu = \omega_\mu^{(0)} \tag{7.19}$$
$$\chi = \chi(\omega_\mu^{(0)})$$

Hence, we are left with effectively same coordinates at each of the Gluon Bundle [29].

Chapter 8

Quarks Transverse Imprecision

8.1 Imprecision in Quark's transverse coordinates

An important point is that quarks are never observed individually, and, thus, cannot have fixed coordinates. The correct coordinates for quarks include transverse quark fluctuations. We believe we know how to do this, the work is still underway for understanding quark fluctuations from first principles. What we have done here is to introduce phenomenlogical transverse fluctuation amplitudes for every quark-gluon vertex, replacing the usual gluon-quark current interaction at the same space-time point

$$\int d^4x \ \bar{\psi}(x)\gamma_\mu A^a_\mu(x)\tau_a\psi(x) \tag{8.1}$$

by

$$\int d^2x'_\perp \int d^4x \ \underline{a(x_\perp - x'_\perp)} \ \bar{\psi}(x')\gamma_\mu A^a_\mu(x)\tau_a\psi(x'), \tag{8.2}$$

with $a(x_\perp - x'_\perp)$ real and symmetric, and $x'_\mu = (x'_\perp, x_L, x_0)$. The probability of finding two quarks separated by a transverse (or impact parameter) distance is then $\varphi(b) = \int \frac{d^2q}{(2\pi)^2} \ e^{iqb} \ |\tilde{a}(q)|^2$.

We chose a deformed gaussian

$$\varphi(b) = \varphi(0)e^{-(\mu b)^{2+\xi}} \tag{8.3}$$

with deformation parameter ξ real and small. A straight forward calculation yields, for small ξ,

$$V(r) \approx \xi\mu(\mu r)^{1+\xi} \tag{8.4}$$

. Perhaps it is important to emphasize again that all asymptotic quark states are hadronic bound states of quarks; and for such a bound state we can specify longitudinal and time coordinates, but not transverse coordinates since they are always fluctuating. The conventional "static quark" approximation used in model binding potential calculations in all non-perturbative amplitudes are plagued with divergences. All non-perturbative amplitudes are plagued with absurdities without taking such "transverse imprecision" into account.

Substituting our potential into a Schrodinger binding equation, using the "quantic" approximation then yields $\mu \sim m_\pi$, with $\xi \approx 0.1$. This is sensible since the maximum fluctuations should be less than m_π^{-1} [27].

Our results encompasses two different lattice calculations, $V \sim r$ and $V \sim r\ln(r)$. All lattice and other model calculations of $q - \bar{q}$ binding correspond to an amplitude containing only one of the two Casimir $SU(3)$ invariants, C_2 or C_3, whereas our amplitude contains both as shown in Section 4, [34, 35]. We used the well-known half century old Eikonal function relation with potential. The minimum bound state energy for the pion shows that most of the pion's mass comes from the gluons forming the GB and relatively little from the quark masses.

Chapter 9

QCD renormalization

9.1 Cluster Expansion

To obtain all configurations between Gluon Bundles and Quark loops, we use a method suggested by Chemists in molecular configurations. Consider a functional $L[A]$ which is acted upon by the linkage operator $exp[\mathfrak{D}]$, with $\mathfrak{D} = -(\frac{i}{2})\int \frac{\delta}{\delta A(\mu)}\mathfrak{D}_c(u-v)\frac{\delta}{\delta A(v)}$. For simplicity, we write

$$\bar{L}[A] = e^{\mathfrak{D}} L[A]. \tag{9.1}$$

To represent $S[A] = e^{\mathfrak{D}} \cdot e^{L[A]}$, we convert $S[A]$ directly to an exponential whose argument is an infinite sum over a set of connected quantities. The representation is

$$S[A] = exp[\sum_{N=1}^{\infty} \frac{Q_N}{N!}], \tag{9.2}$$

where the $Q_N[A]$ are connected functionals, initially defined as

$$\begin{aligned} Q_N[A] &= e^{\mathfrak{D}} L^N[A]|_{connected} \\ &= \prod_{i>j=1}^{N} e^{\mathfrak{D}_{ij}} \cdot \prod_{i=1}^{N} e^{\mathfrak{D}_{\mathrm{i}}} L[A_i]|_{connected, A_i=A}, \\ &= \prod_{i>j}^{N} e^{\mathfrak{D}_{\mathrm{ij}}} \cdot \prod_{i=1}^{N} \bar{L}[A_i]|_{connected, A_i=A} \end{aligned} \tag{9.3}$$

The subscript "connected" indicates that at least one linkage must be retained between any and each pair of $L[A_k]$ terms. For $N = 1$, $Q_1[A] = \bar{L}[A]$. Explicit Q_N forms are found by using lagrange multiplier λ such that $L \to \lambda L$, then $Q_N \to \lambda^N Q_N$. $S[A]$ becomes

$$exp[\sum_{n=1}^{\infty} \frac{\lambda^n Q_n}{n!}] = e^{\mathfrak{D}} \cdot e^{\lambda L} \tag{9.4}$$

or

$$\sum_{n=1}^{\infty} \frac{Q_n}{n!} = ln[e^{\mathfrak{D} \cdot e^{\lambda L}}] \tag{9.5}$$

Each Q_N can be obtained by applying $(\partial/\partial\lambda)^N|_{\lambda=0}$ on above. For example, $Q_1 = [e^{\mathfrak{D} \cdot L e^{\lambda L}}[e^{\mathfrak{D} \cdot e^{\lambda L}}]]|_{\lambda=0} = e^{\mathfrak{D}} \cdot L = \bar{L}$. Figure 9-1. For Q_4, we obtain the following

$Q_1 = e^{\hat{\mathfrak{D}} \wedge} L[A] =$  $= \bar{L}[A]$

Figure 9-1: Graphical expansion of Q_1

expansion as shown in figure 9-2. The multiplicative factor for each term can be obtained by direct counting or combinatorics [23].

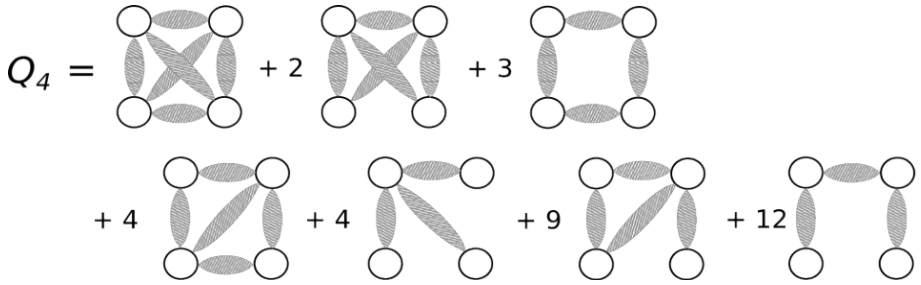

Figure 9-2: Graphical expansion of Q_4

9.2 Renormalization

The radiative corrections of QCD enter when there is momentum transfer between one quark and another quark, where momentum transfer passes through intemediate GBs and/or closed quark loops.

We use an exact functional cluster expansion described in Chapter 2.5 of [23]. In our particular choice of renormalization, we choose $\delta^2\ell = \kappa$, where δ represent point where GB connects to a quark loop. The quark loop, ℓ, has the expected UV log divergence and κ is a finite positive constant, figure 9-3.

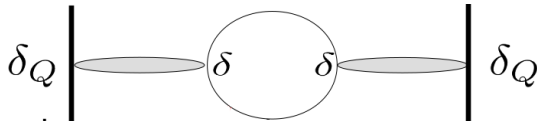

Figure 9-3: We chose a renormalization scheme where two connections of Gluon Bundles, δ, multplied by a quark loop with logarithmic divergence, ℓ are set equal to a finite quantity κ, to be determined by experiments.

With this particular choice if renormalization, only GB chain graphs are non-zero. All other closed loops entering into the functional cluster expansion vanish. In figure 9-2, only the last term will be non-zero. These GB chain graphs form a geometric series which can be summed, and is everywhere finite. See figure 9-4.

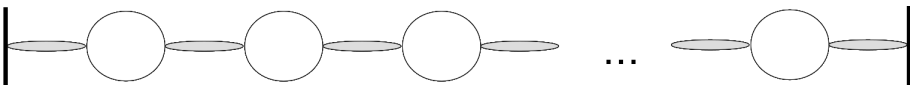

Figure 9-4: We set $\delta^2 \cdot \ell = \kappa$, where κ is assumed finite and determined by experiment. This simplifies all posible loop connections with Gluon Bundles to only the straight chains. This is the first attempt at renormalization, and, thus far, compares well with experiments.

The real radiative corrections in QCD are formed from Gluon Bundles and Quark-Antiquark loops. We are in position now to calculate scattering amplitudes between Quark/(anti)Quark processes.

All the basic radiative correction structure of non-perturbative QCD comes from interacting closed-quark-loops with GB's. A single dressed quark has an amplitude

proportional to

$$N \int d[\chi] e^{i\frac{\chi^2}{4}} (det(gf \cdot \chi)^{-\frac{1}{2}}) e^{\hat{\mathfrak{D}_A}} \cdot G_c[A] e^{L[A]}|_{A\to 0}, \tag{9.6}$$

While two scattering quarks are described by

$$N \int d[\chi] e^{i\frac{x\chi^2}{4}} (det(gf \cdot \chi)^{-\frac{1}{2}}) e^{\hat{D}_A} G_c^{(1)}[A] G_c^{(2)}[A] e^{L[A]}|_{A\to 0}, \tag{9.7}$$

where $\hat{\mathfrak{D}}_A = \frac{i}{2} \int \frac{\partial}{\partial A} (gf \cdot \chi)^{-1} \frac{\partial}{\partial A}$.

9.3 Quark self-energy

Every GB exchanged is represented by the linkage operator connecting the two $G_c[A]$'s to each other, and the $G_c[A]$'s to $L[A]$. Explicit calculation shows that all self-energy graphs vanish either by asymmetry of the $(f \cdot \chi)^{-1}$ color and indices or by explicit loop integration. See Figure 9-5. All self energies of a quark are exactly 0. Of course, we cannot make comments on individual quark masses, the quark line in Figure 9-5 includes its transverse imprecision as discussed in Section 8.1. In other words, realistic quarks must be in bound states.

Non-perturbative QCD turns out to be far simpler than QED.

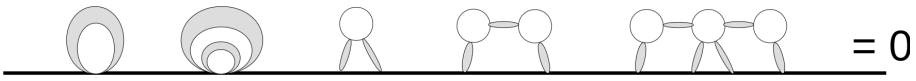

Figure 9-5: All self energy graphs with Gluon Bundles are zero, 0.

Chapter 10

Masses and Confinement Scale(s)

10.1 QCD confinement scale(s)

In the formulation in 8.1, the confinement mass μ appears in the transverse fluctuation probability $\varphi(b)$. Values of $b > 1/\mu$ give negative contributions to any Fourier transform of powers of $\varphi(b)$. We shall use a simpler procedure here to obtain an approximate equation for the bound state energy, m_{bs}.

$$\varphi(b) = \varphi(0)\ e^{-(\mu b)^{2+\xi}}, \tag{10.1}$$

The transverse fluctuations of the bound quarks inside a bound state particle cannot be larger than the Compton wavelength of that particle. The deformation parameter ξ in Eq. 10.1 is the origin of quark binding in section 8.1. For a pion, b is the transverse separation of a $q - \bar{q}$ pair forming a pion, and μ is the mass scale such that transverse fluctuations larger than μ^{-1} give little contribution. Deformation parameter ξ is a small, real and positive number, of the order of 0.1 in a pion [32].

Of note is that the G^{23}_{34} Meijer function's in section 4.2 mixes partonic variables $m, \hat{s}$ with Eq 10.1. This is a prediction in Brodsky and company's approach in [49, 11].

The corresponding potential arrived through Eikonal function, χ of chapter 2.4, is that of Eq. 8.4,

$$V(r) \simeq \xi\mu(\mu r)^{1+\xi}, \tag{10.2}$$

where μ was taken to be on the order of the pion mass, m_π.

For larger bound states, μ is that larger particle's mass, m_{BS}. Deformation parameter is expected to be smaller than $\xi < \xi_\pi$ used for the pion. In our formulation, 3 quarks bound states have $xi_{nucleon} \sim 0.1$. The Fourier transform of $\varphi(b)$ is then

$$exp[-\vec{q}^{\,2}/4m_p^2], \tag{10.3}$$

where m_p is the proton's mass. Eq. 10.3 is of the form of momentum space fall-off suggested in recent Brodsky and company's light-front analysis [49, 11].

For a simplified analysis, we replace the r_{ij} in each of the $q-\bar{q}$'s $V(r)_{ij}$ with $1/m_\pi$. We can now write energy of a bound particle, E_0 as,

$$E_0 \rightarrow m_{BS} \simeq n_q m_q + \xi \sum_q m_{BS} \left(\frac{m_{BS}}{m_\pi} \right)^{1+\xi}, \tag{10.4}$$

where $\sum_q$ represents the number of pairwise q and/or $\bar{q}$ interactions. One them obtains

$$m_{BS} \simeq n_q m_q + \frac{n_q(n_q-1)}{2} m_{BS}\ \xi \left(\frac{m_{BS}}{m_\pi} \right)^{1+\xi}; \tag{10.5}$$

and since ξ is expected to be $\ll 1$, Eq. 10.5 simplifies further to

$$\xi \simeq [1 - \frac{n_q m_q}{m_{BS}}] \cdot \left(\frac{1}{\frac{n_q(n_q-1)}{2}(\frac{m_{BS}}{m_\pi})} \right). \tag{10.6}$$

What we have is that μ is mass of the bound state m_{BS} and must be less than the Compton wavelength of the particle. This in term determines the deformation parameter ξ. The reverse is also true: if we know ξ, we can determine m_{BS}. The mass parameters in later chapter 11 and chapter 12 can be determined if we have ξ. Some values for bound states have been listed in Table B.1 in Appendix B.

10.2 Nuclear physics from QCD

In the same light, nucleon binding is examined. Here is the first (to our knowledge) example of nucleon binding, for a model deuteron, from basic QCD [28]. We have performed a qualitative model, without electrical charge and nucleon spins which can always be added in, to describe the essence of Nuclear Physics. Assuming an average quark for ease of calculation, an attractive potential is obtained [27, 24]. Quark binding takes place for $r_{ij} \approx m_\pi^{-1}$, but for nucleon binding that takes place at larger distances. Extraction and regularization of the logarithmic UV divergence loop will

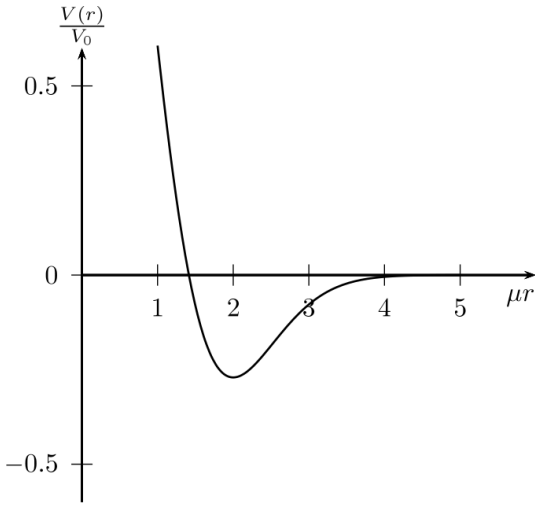

Fig. 3. Nucleon potential with $V_0 = c(\frac{g_R^2}{4\pi})\mu$.

Figure 10-1: Nucleon nucleon binding is mediated by the exchange of Gluon Bundles supporting one or more closed quark loops. The change in sign is the important factor that enables binding to occur.

contribute two essential features.

1. The loop stretches, so distances larger than m_π^{-1} can easily enter

2. It provides a crucial change of sign for the effective n-n binding potential, figure 10-1, [27].

   We expect and hope that nuclear physicists will employ such effective potentials to discuss heavier nuclei. A model deuteron is constructed from first principles in article [28]. See Figure 10-2.

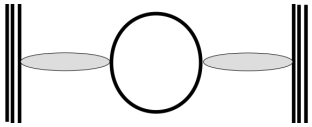

Figure 10-2: Nucleon nucleon binding is mediated by the exchange of Gluon Bundles with a quark loop that is able to stretch to distances greater than that of a pion. The change in sign in the derived potential in Figure 10-1 provides the crucial ingredient for binding to occur.

Chapter 11

QCD Scattering Amplitude

11.1 Eikonal approximation

The scattering amplitude we obtain from the eikonal is:

$$T_{eikonal}(s,t;g^2) = \frac{is}{2m^2}\int d^2b e^{iqb}[1-e^{i\chi_0(s,b)}] \tag{11.1}$$

The relation between $\varphi\tilde{(}b)$ and the eikonal, χ is given by

$$e^{i\chi(s,b)} = \mathfrak{N}'\int_0^\infty dRR^3 e^{iR^2/4+ig\tilde{\varphi}(b)/R} \tag{11.2}$$

if we used our $R^2 = \sum_a \chi^2$ approximation. The amplitude can be calculated exactly, however, at this stage, we use our intuitive understanding that all the angles in the color space are the same. The s dependence will be part of our normalization for the δ that connects a real physical quark to a gluon bundle, this takes the form $(m/E)^{2p}$ where p is to be extract from experiments.

11.2 Scattering Amplitude

With our renormalization scheme, and a first rough pass as averaging $\sum \chi^2$'s by an average R^2, we calculate quark/(anti)quark scattering amplitude, T.

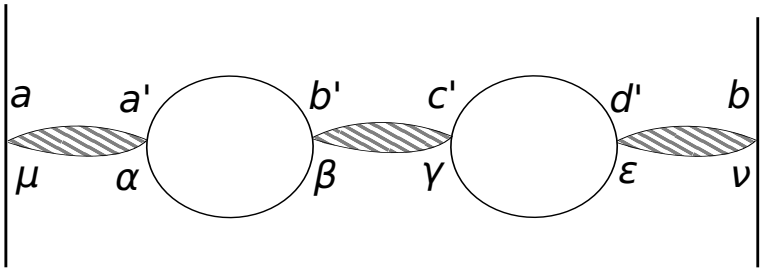

Figure 11-1: Two averaged quarks connected by GB's and two loops.

For ease of presentation, let's calculate a two loop chain graph scattering amplitude, T, in Fig. 11-1. T is proportional to

$$
\begin{aligned}
T = \quad & \int_0^s \mathrm{d}s_1\, u'_\mu(s_1)\, \Omega_a(s_1) \int_0^{\bar{s}} \mathrm{d}\bar{s}_1\, \bar{u}'_\nu(\bar{s}_1)\, \bar{\Omega}_b(\bar{s}_1) \cdot \int_0^t \mathrm{d}t_1\, v'_\alpha(t_1)\, \hat{\Omega}_{a'}(t_1) \qquad (11.3)\\
\cdot \quad & \int_0^t \mathrm{d}t_2\, v'_\beta(t_2)\, \hat{\Omega}_{b'}(t_2) \cdot \int_0^{\bar{t}} \mathrm{d}\bar{t}_1\, \bar{v}'_\gamma\, \breve{\Omega}_{c'}(\bar{t}_1) \cdot \int_0^{\bar{t}} \mathrm{d}\bar{t}_2\, v'_\epsilon(\bar{t}_2)\, \breve{\Omega}_{d'}(\bar{t}_2)\\
\cdot \quad & \int \mathrm{d}^2 y'_\perp\, \mathfrak{a}(y_\perp - y'_\perp) \cdot \int \mathrm{d}^2 \bar{y}'_\perp\, \mathfrak{a}(\bar{y}_\perp - \bar{y}'_\perp) \cdot \int \mathrm{d}^2 x'_\perp\, \mathfrak{a}(x_\perp - x'_\perp)\\
\cdot \quad & \int \mathrm{d}^2 x''_\perp\, \mathfrak{a}(x_\perp - x''_\perp) \cdot \int \mathrm{d}^2 \bar{x}'_\perp\, \mathfrak{a}(\bar{x}_\perp - \bar{x}'_\perp) \cdot \int \mathrm{d}^2 \bar{x}''_\perp\, \mathfrak{a}(\bar{x}_\perp - \bar{x}''_\perp)\\
\cdot \quad & \delta^{(4)}(y' - u(s_1) - x' + v(t_1)) \cdot \delta^{(4)}(x'' - v(t_2) - \bar{x}' + \bar{v}(\bar{t}_1)) \cdot \delta^{(4)}(\bar{x}'' - \bar{v}(\bar{t}_2) - \bar{y}' + \bar{u}(\bar{s}_1))\\
\cdot \quad & [f \cdot \chi(y' - u(s_1))]^{-1}|^{aa'}_{\mu\alpha} \cdot [f \cdot \chi(\bar{x}' - \bar{v}(\bar{t}_1))]^{-1}|^{b'c'}_{\beta\gamma} \cdot [f \cdot \chi(\bar{y}' - \bar{u}(\bar{s}_1))]^{-1}|^{d'b}_{\epsilon\nu},
\end{aligned}
$$

where the $\mathfrak{a}(z_\perp - z'_\perp)$ represent the probability amplitudes of each quark to be found at a perpendicular distance $z'_\perp$ about its average. The probability of an individual GB delivering momentum q is given by $\tilde{\varphi}(q) = [\tilde{\mathfrak{a}}(q)]^2$. The δ-functions of Eq. (11.3) shows *Effective Locality*, and $z'_\mu = (z_0, z_L; z'_\perp)$, where 0 is time-like and L is longitudinal components. The three $(f \cdot \chi)^{-1}$'s are the three GB's in T. The x and $\bar{x}$ are the space-time coordinates of each loop. The y and $\bar{y}$ coordinates represent each quark, with corresponding Fradkin functional variables $u(s')$ and $u(s')$.

Now perform the following steps:

1. Suppress the primes in the arguments of each $(f \cdot \chi)^{-1}$; the justification for this step is given in Appendix B of Ref. [30].

2. Assume that $[f \cdot \chi(\bar{x} - \bar{v}(\bar{t}_1))]^{-1}$ is labeled only by its transverse arguments, an

assumption made for convenience, which is consistent with the final results of this exercise.

3. Write an integral representation for each of the time-like and longitudinal δ-functions of Eq. (11.3), thereby introducing the Fourier variables $q_0, q_L, p_0, p_L, k_0, k_L$. Assume the two quarks of Fig. 11-1 are scattering at high energy and use the Eikonal Model. This removes the need for an integration over the Fradkin u- and $\bar{u}$-dependence. The result is that the Fourier variables $q_0, q_L, p_0, p_L, k_0, k_L$ vanish, leaving only transverse $q_\perp, p_\perp, k_\perp$ dependence.

4. Write Fourier representations for the remaining three transverse delta-functions of Eq. (11.3), and calculate the integrals $\int \mathrm{d}^2 y'_\perp \cdot \int \mathrm{d}^2 \bar{y}'_\perp \cdot \int \mathrm{d}^2 x'_\perp \cdot \int \mathrm{d}^2 x''_\perp \cdot \int \mathrm{d}^2 \bar{x}'_\perp \cdot \int \mathrm{d}^2 \bar{x}''_\perp$ to obtain factors of $\tilde{\varphi}(q) \cdot \tilde{\varphi}(p) \cdot \tilde{\varphi}(k)$ where all previous $z'_\perp$ are effectively replaced by $z_\perp$.

5. Calculate $\int \mathrm{d}^2 x_\perp \cdot \int \mathrm{d}^2 \bar{x}_\perp$ and find that $p_\perp = k_\perp = q_\perp$, so that there is but one transverse integral, $\int \mathrm{d}^2 q_\perp \equiv \int \mathrm{d}^2 q$ remaining.

The three transverse δ-functions multiplying the last line of Eq. (11.3) can be used to re-write the $[f \cdot \chi(\bar{x} - \bar{v}(t_1))]^{-1}$ term as

$$\left[f \cdot \chi \left(\frac{1}{2} [x - v(t_2) + \bar{x} - \bar{v}(\bar{t}_1)] \right) \right]^{-1} \tag{11.4}$$

$$\Rightarrow \quad \left[f \cdot \chi \left(\frac{1}{2} [y - u(s_1) + v(t_1) - v(t_2) - \bar{v}(\bar{t}_1) + \bar{v}(\bar{t}_2) + \bar{y} - \bar{u}(\bar{s}_1)] \right) \right]^{-1},$$

and, as explained in Ref. [30, 33], in the Center of Mass (CM) of the scattering quarks, with the zero of time chosen as that time when both quarks' longitudinal coordinates are zero, the Eikonal Model effectively replaces $y - u(s_1)$ by $y_\perp$, and $\bar{y} - \bar{u}(\bar{s}_1)$ by $\bar{y}_\perp$. This replaces Eq. (11.4) by

$$\left[f \cdot \chi \left(\frac{1}{2} [y_\perp + \bar{y}_\perp + \Delta v - \Delta \bar{v}] \right) \right]^{-1}, \tag{11.5}$$

where $\Delta v = v(t_1) - v(t_2)$, and $\Delta \bar{v} = \bar{v}(\bar{t}_1) - \bar{v}(\bar{t}_2)$. With the CM value of the transverse

vectors $y_\perp + \bar{y}_\perp = 0$, Eq. (11.5) reduces to

$$\left[f \cdot \chi \left(\frac{1}{2} [\Delta v - \Delta \bar{v}] \right) \right]^{-1}. \tag{11.6}$$

The remaining transverse integral over $\mathrm{d}^2 q_\perp$ has

$$e^{iq \cdot [y_\perp - \bar{y}_\perp + \Delta v + \Delta \bar{v}]}, \tag{11.7}$$

in its integrand, where $y_\perp - \bar{y}_\perp = \vec{b}$ is the impact parameter. The $(f \cdot \chi)^{-1}$ of Eq. (11.6) must now be included as part of Fradkin's v and $\bar{v}$-integrals. For this, we write a Fourier representation of Eq. (11.6) as

$$\int \frac{\mathrm{d}^2 K}{(2\pi)^2} \, \widetilde{\mathcal{F}}(K) \, e^{i \frac{K}{2} [\Delta v - \Delta \bar{v}]}, \tag{11.8}$$

and note that the UV divergent part of the Fradkin integrals over both loops, $\int \mathrm{d}[v] \cdot \int \mathrm{d}[\bar{v}]$, is proportional to the product

$$\left[-\lambda \, \delta_{\alpha\beta} \, (q + \frac{1}{2} K)^2 \, \ell \right] \cdot \left[-\lambda \, \delta_{\gamma\epsilon} \, (q - \frac{1}{2} K)^2 \, \ell \right], \quad \ell = \ln(1/m) \tag{11.9}$$

using our original approximation for the spin dependence of each loop. Note that the color indices of each side of the loop are forced to be identical in the divergent limit of the loop.

Without its K-dependence, Eq. (11.9) is just given by the product of the two loops' q^2-factors. That K-dependence appears in the form of a sum over products of polynomial dependence on K components, multiplying the transform $\widetilde{\mathcal{F}}$. We now take the inverse transform with

$$\tilde{\mathcal{F}}(K) = \int \mathrm{d}^2 B \, e^{-iK \cdot B} \, [f \cdot \chi(B)]^{-1}. \tag{11.10}$$

Each K-component K_α can be expressed as a derivative with respect to B_α of the inverse transform, $K_\alpha \to i \frac{\partial}{\partial B_\alpha}$. An integration-by-parts transforms this and all such derivatives from the polynomial K-dependence of Eq. (11.9) into one or more deriva-

tives operating upon $[f \cdot \chi(B)]^{-1}$. The $\int \mathrm{d}^2K$ can now be immediately, yielding $\delta^{(2)}(B)$. The result of all the K-dependence of Eq. (11.9) is a group of derivatives taken at $B = 0$.

We have not yet allowed the small space-time interval of the $(f\cdot\chi)^{-1}$ of this central GB to vanish, in conjunction with the loop UV divergences becoming infinite. Each of the small space-time volume is completely independent of its neighbors such that the $\frac{\delta}{\delta B_\alpha}$ operating on them. We are free to define how the limit is to be taken and, we shall, take the simplest case of a "flat" volume without any curvature. Each and every derivative on this flat volume vanishes as $B \to 0$. To put it in another way, any curvature introduces a scale; and there is no relevant scale to adopt.

The contribution of this two-loop chain is then proportional to the product of two groups of q-factors, one from each loop, separated by the matrix quantity $[f \cdot \chi(0)]^{-1}|^{b'c'}_{\beta\gamma}$ which we now replace by the simplified expression

$$(-\lambda q^2 \delta_{\alpha\beta})(-\lambda q^2 \delta_{\gamma\epsilon})\kappa^2. \tag{11.11}$$

This result of the form of Eq. (11.11) will hold for every 'interior' GB of the chain. For example, the three-loop amplitude has four $(f \cdot \chi)^{-1}$ factors where the central two may both be re-written as

$$\sum_{\beta,c'} [f \cdot \chi(0)]^{-1}|^{b'c'}_{\alpha\beta} \cdot [f \cdot \chi(0)]^{-1}|^{c'd'}_{\beta\gamma}, \tag{11.12}$$

or as $[f \cdot \chi(0)]^{-2}|^{b'd'}_{\alpha\gamma}$.

Thus, the result for a chain with n 'interior' GBs yields a term proportional to $[f \cdot \chi(0)]^n|^{b'd'}_{\alpha\gamma}$ which is inserted between the two 'exterior' GBs, $[f \cdot \chi(y_\perp)]^{-1}|^{aa'}_{\mu\alpha}$ on the left and $[f \cdot \chi(\bar{y}_\perp)]^{-1}|^{d'b}_{\epsilon\nu}$ on the right, multiplied by the remaining q-dependence, and integrated over all transverse q. With $a(q^2) = \lambda\, q^2\, \kappa\, g\, \tilde{\varphi}(q)$, all together one has, upon summing over all interior loops which effectively form a geometric series, and

including the amplitude with but one loop,

$$
\begin{aligned}
T_{chain} = \quad & [f\cdot\chi(y_\perp)]^{-1}\big|_{\mu\alpha}^{aa'}\cdot\, ga(q^2)\tilde{\varphi} \\
& \times\left[1+ia(q^2)\,[f\cdot\chi(0)]^{-1}-a(q^2)^2\,[f\cdot\chi(0)]^{-2}-ia(q^2)^3\,[f\cdot\chi(0)]^{-3}+\cdots\right]_{\alpha\beta}^{a'b'} \\
& \cdot\,[f\cdot\chi(\bar{y}_\perp)]^{-1}\big|_{\beta\nu}^{b'b},
\end{aligned}
\tag{11.13}
$$

or, suppressing matrix indices,

$$
T_{chain} = [f\cdot\chi(y_\perp)]^{-1}\cdot ga(q^2)\tilde{\varphi}\,\left[\frac{1+ia(q^2)[f\cdot\chi(0)]^{-1}}{1+a(q^2)^2\,[f\cdot\chi(0)]^{-2}}\right]\cdot[f\cdot\chi(\bar{y}_\perp)]^{-1}. \tag{11.14}
$$

Eq. (11.14) can be replaced by

$$
T_{chain} = ga(q^2)\tilde{\varphi}\,[f\cdot\chi(y_\perp)]^{-1}\cdot[f\cdot\chi(0)]^2\,\left[\frac{1+ia(q^2)[f\cdot\chi(0)]^{-1}}{[f\cdot\chi(0)]^2+a(q^2)^2}\right]\cdot[f\cdot\chi(\bar{y}_\perp)]^{-1}. \tag{11.15}
$$

Since the indices α and β of $\chi^a_{\alpha\beta}(0)$ are transverse, all components of $\chi(0)$ can be chosen as real. With f^{abc} real, $[f\cdot\chi(0)]^2$ is positive, and the denominator of Eq. (11.15) is never zero. The $\chi(0)$ contribution to the amplitude is then proportional to

$$
g^2\int \mathrm{d}^2q\, e^{iq\cdot\vec{b}}\cdot[f\cdot\chi(y_\perp)]^{-1}\cdot I(q^2,g^2)\cdot[f\cdot\chi(\bar{y}_\perp)]^{-1} \tag{11.16}
$$

or

$$
g_R^2(q^2) = g^2\; I(q^2,g^2)\; q^2[\tilde{\varphi}(q)]^2\;\lambda\kappa \tag{11.17}
$$

with

$$
I(q^2,g^2) = \mathcal{N}\int \mathrm{d}^4\chi(0)\;\det[f\cdot\chi(0)]^{-\frac{1}{2}}\,e^{\frac{i}{4}\chi(0)^2}\,\frac{[f\cdot\chi(0)]^2}{[f\cdot\chi(0)]^2+[\lambda\kappa g q^2\tilde{\varphi}]^2}, \tag{11.18}
$$

since the integral $\int \mathrm{d}^n\chi(0)$ over an odd function of $[f\cdot\chi(0)]^{-1}$ vanishes.

There is no divergence in the integral of Eq. (11.16) for any value of q^2. The Fourier transform of this integral corresponds to q^2 dependence in momentum space.

This factor will be present in every interacting quarks processes, and as such, can be considered as the renormalized color-charge dependence of this Model renor-

malization, as the 'renormalized' charge which appears in the scattering of a pair of quarks and/or anti-quarks, at q-values somewhat different from those obtained from simple one-GB exchange. Integrals over this quantity are then finite by virtue of the exponential cut-off appearing in $\tilde{\varphi}(q)$, which is (slightly) less strong than Gaussian, reflecting the basic structure of confinement in this Model of Realistic QCD. This chain-graph Bundle structure will be repeated in all of the correlation functions. The integrations over coordinate components are all finite even if complicated. Methods of Random Matrix theory [34, 31] can be used to evaluate multiple-chain contributions to high-energy hadronic reactions, in particular elastic pp scattering.

For ease of computation, and to demonstrate the origin and appearance of the familiar "diffraction dip" in the (momentum-transfer)^2 region of $\frac{m_p^2}{2}$, we adopting two intuitive, qualitative approximations for the exchange of a single GB-loop chain between a pair of scattering quarks, each bound into a different proton. For momentum exchange much smaller than the CM energies, individual proton's quarks interactions are suppressed.

The first approximation is to represent the amplitude of a single chain by its first two terms, as pictured in Fig. 11-2. The second approximation is to evaluate $\int \mathrm{d}^n\chi(0)$ by treating χ^a as a vector in color space, with magnitude $R = \sqrt{\sum_a (\chi^a)^2}$, greatly simplified by suppressing all of the normalized integrations over such angles, and retaining only the normalized integration over R. This permits evaluations with

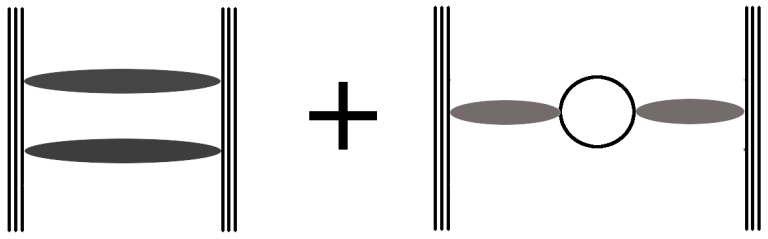

Figure 11-2: First two terms of complete amplitude. A Gluon Bundle term (two bundles because one bundle is anti-symmetric) plus One-Closed-Quark-Loop term

experiments, namely, the differential cross section of elastic proton-proton scattering.

11.3 Differential Cross Section

Elastic differential cross section is given by

$$\frac{d\sigma}{dt} = \frac{m^4}{16\pi p^2 E^2}|T_{summed}|^2 \tag{11.19}$$

The amplitude for two Gluon Bundles is

$$\frac{d\sigma}{dt} = k[-12\frac{\beta_{ext}g^2}{4\pi}(\frac{m}{E})^{2p}(\frac{m}{E})^{2p}exp(-\frac{3}{8}\frac{x}{m^2})]. \tag{11.20}$$

Adding in the one loop amplitude gives

$$\begin{aligned}\frac{d\sigma}{dt} = k[&- 12\frac{\beta_{ext}g^2}{4\pi}(\frac{m}{E})^{2p}(\frac{m}{E})^{2p}exp(-\frac{3}{8}\frac{x}{m^2}) \\ &+ \ 9\frac{\beta_{ext}g^2}{4\pi}(\frac{m}{E})^{2p}4\pi\lambda\bar{\kappa}\frac{x}{m^2}exp(\frac{-x}{2m^2})]^2.\end{aligned} \tag{11.21}$$

The factor k absorbed all physical constants and converted to the experimental data unit mb/GeV. The β's come from the $exp[i\beta/4] = exp[i\sum_a \chi^2/4]$ term and can be calculated exactly with random matrix methods. (β_{ext} connects to physical quarks at the ends of the chain, and β_{int} connects to the virtual interior quark loops.) The factor 12 in front of the Gluon Bundle term represents 12 ways two GB's can be arranged between three and three bound quarks, see Figure 11-2. The factor 9 is the number of ways a single loop chain can connect between three and three bound quarks.

For the infinite loops summed, see Figure 12-9, we calculated the differential cross-

section to be,

$$\begin{aligned}\frac{d\sigma}{dt} = k[&- 12\frac{\beta_{ext}g^2}{4\pi}(\frac{m}{E})^{2p}(\frac{m}{E})^{2p}exp(-\frac{3}{8}\frac{x}{m^2}) \\ &+\ 9\frac{\beta_{ext}g^2}{4\pi}(\frac{m}{E})^{2p}4\pi\lambda\bar{\kappa}\frac{x}{m^2}exp(\frac{-x}{2m^2}) \\ &+\ 9(6\times 6\times 2\times 2)^2(\frac{\beta_{int}g^2}{4\pi})(\frac{m}{E})^{2p}(4\pi\lambda\bar{\kappa}) \\ &\left(\frac{1}{2}g\cdot a(x)\tilde{\varphi}(x)^2\times(\frac{(\frac{a(x)6-7a(x)^2}{\beta_{int}^2})-(\frac{5a(x)^4}{\beta_{int}}+\frac{3}{\beta_{int}^3})}{a(x)^8+\frac{1}{\beta_{int}^4}+\frac{2a(x)^4}{\beta_{int}^2}})\right)]^2\end{aligned} \tag{11.22}$$

where $a(x) = gx\kappa\tilde{\varphi}(x)$, x is the momentum transfer q^2, β_{ext} represents connections to exterior (real) quark line, while β_{int} represents connections to interior quark loops. $\tilde{\varphi}(x) = exp[-i(x/m)^{2-\eta}]$ is the fourier transform of our transverse quark imprecision distribution, $\varphi(b)$ in equation 8.3 where η is the inverse of ξ. For simplicity, we shall let experiments determine β, while coupling g, renormalizations κ, p, and m must be extracted from experiments.

Chapter 12

Comparison with High Energy scattering experiments

12.1 Elastic pp-scattering

In high energy hadron scattering, pp-scattering in particular, there has always been a 'diffraction dip' that was difficult to explain and certainly not from first principles. There are form factors, or other methods attempted. For us, we calculate the differential cross section from, intuitively trying a GB exchanged between two hadrons (3 quarks that are not breaking up) and a GB-virtual quark loop-GB configuration. Just to get an intuitive understanding. Low and behold, we have a diffraction dip as seen in experiments. It comes from quark-GB-quark and quark-GB-virtualquarkloop-GB-quark, Figure 12-1 and Figure 12-2, [33].

The contribution from purely GB's exchanged between two nucleons provide an amplitude with exponential fall off, while the one-loop-term provides a rising function, figure 12-1, that, when both combined explains the diffraction dip. The exact form that includes infinite sum of all chain loops are currently underway. We expect favorable comparison with the experimental measurements [2, 3, 4, 8].

The δ_q in our amplitude that connects to physical quark lines have units of time, giving us inverse eenergy relation. Raising $1/E$ to the first power provided too strong an energy dependence for positions of the dips. With δ_q proportional to $(1/m)(m/E)^p$,

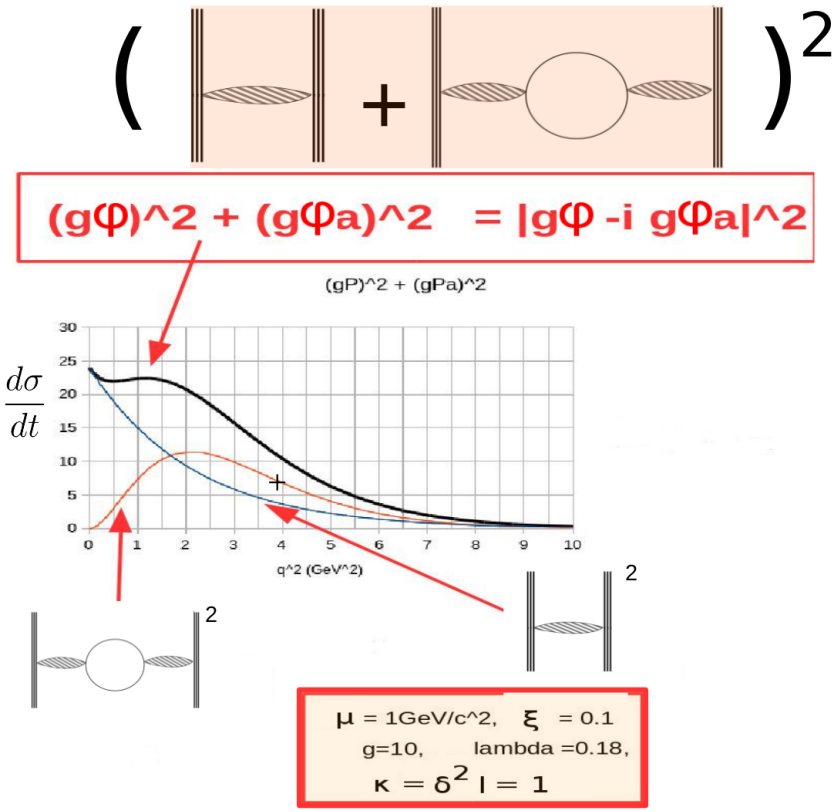

(H.M.Fried, Y.Gabellini, T.Grandou, Y-Ming Sheu, PHT. Annals of Physics 2015)

Figure 12-1: Elastic differential cross-section is most simply calculated from exchange of Gluon Bundles between hadrons and exchange of Gluon Bundles between hadrons with an additional one-quark-loop. The restriction to one loop is a first approximation.

the power p can be deduced from data. See figure 12-3. The parameters coupling g, (re)normalization constants κ and p, and m, mass scale, β's will be determined from experiment. Note that the β's can be computed exactly with random matrix methods, but for now, we shall let experiments give us this value.

12.2 Elastic Scattering Amplitude with Gluon Bundle and One quark loop term

Amplitude for gluon bundles and one loop between two hadrons is given by Eq. 11.21, where each hadron is comprised of 3 average quarks. See figure 12-3,12-4,12-5,12-6,12-

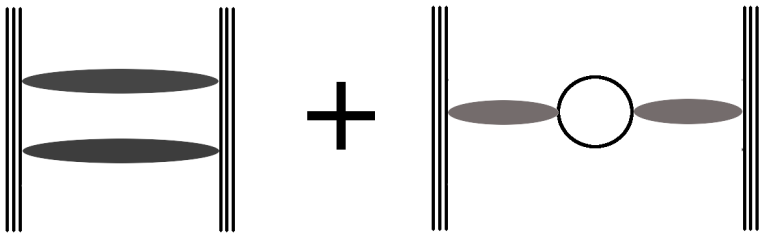

Figure 12-2: Gluon Bundles term (two bundles because one bundle is anti-symmetric) plus Gluon-Bundle-One-Closed-Quark-Loop term

7 and 12-8. The parameters resulted from this amplitude are

$$\begin{aligned} g &= 2.9 \\ m &= 2m_\pi \\ p &= 0.01 \\ \beta_{ext} &= 3.0 \\ \kappa &= 0.0296 \end{aligned} \tag{12.1}$$

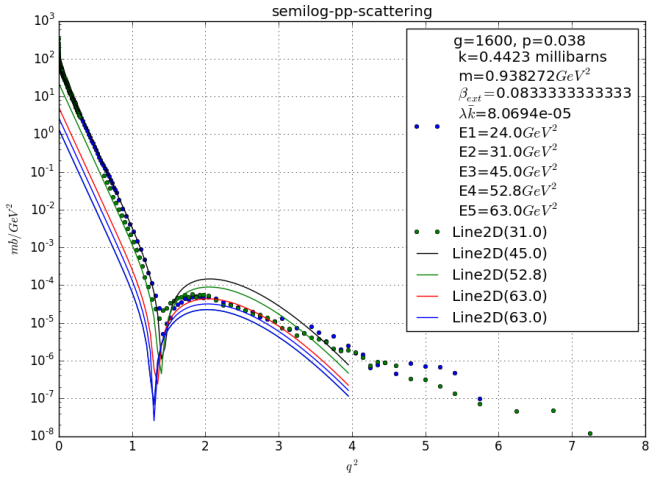

Figure 12-3: Early comparisons of Gluon Bundle exchanges and the one-loop-term amplitude compares well with Intersecting Storage Ring data of elastic pp-scattering. Data points are in small circular points. Our calculations are solid lines. There is the expected movement of the dip to smaller q^2 as energy, $\sqrt{s}$ is increased, [2, 3, 4, 8].

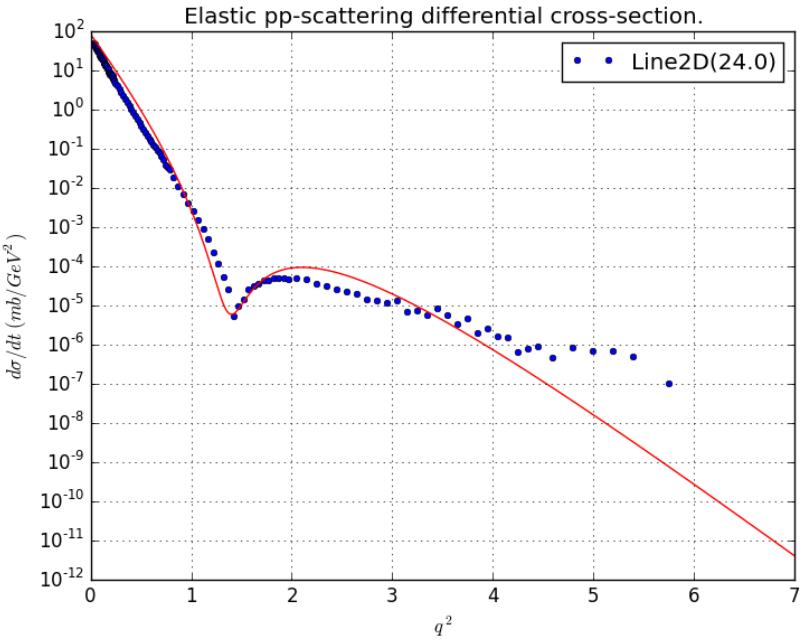

Figure 12-4: 24 GeV ISR fit using amplitude with gluon bundles and one loop term.

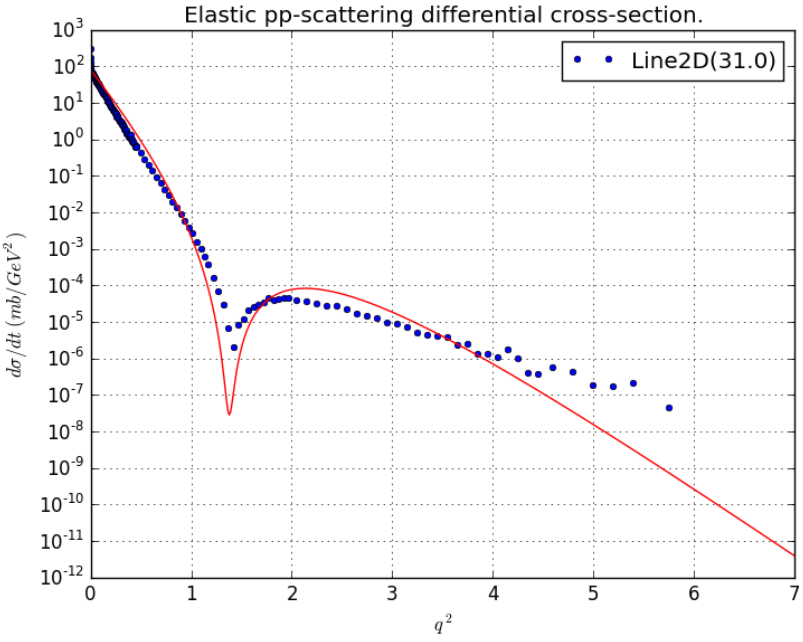

Figure 12-5: 31 GeV ISR fit using amplitude with gluon bundle and one loop term.

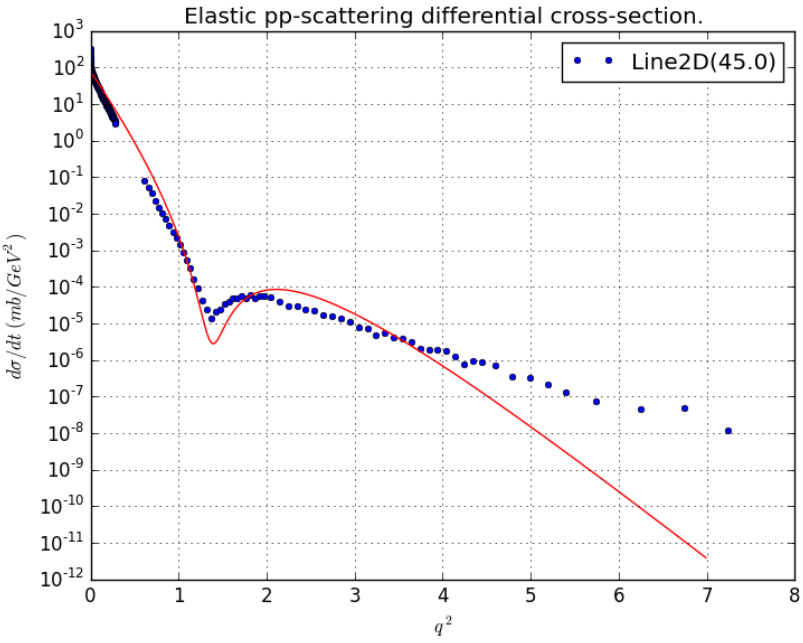

Figure 12-6: 45 GeV ISR fit using amplitude with gluon bundle and one loop term.

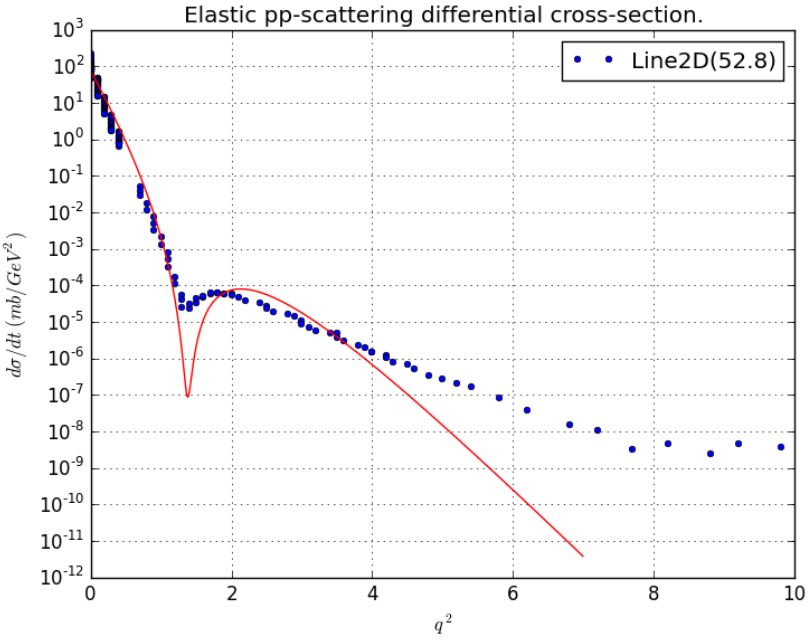

Figure 12-7: 53 GeV ISR fit using amplitude with gluon bundle and one loop term.

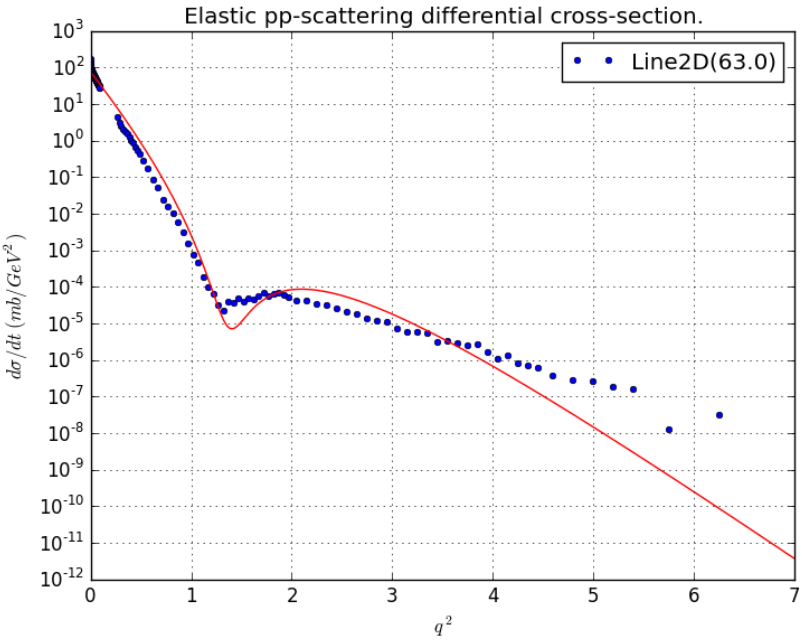

Figure 12-8: 63 GeV ISR fit using amplitude with gluon bundle and one loop term.

12.3 Elastic Scattering Amplitude with Gluon Bundle and Infinite summed loop chains

For the full elastic scattering amplitude given by Eq. 11.22, there are 9 possible ways for the left hand side quarks in a proton to connect to the right hand side quarks of the other proton, corresponding to 3 x 3 different ways the chain can be exchanged. Consider the left hand side quark touching the external quark, there are 3 colors and 2 transverse choices that can be made for the left hand side of that GB.

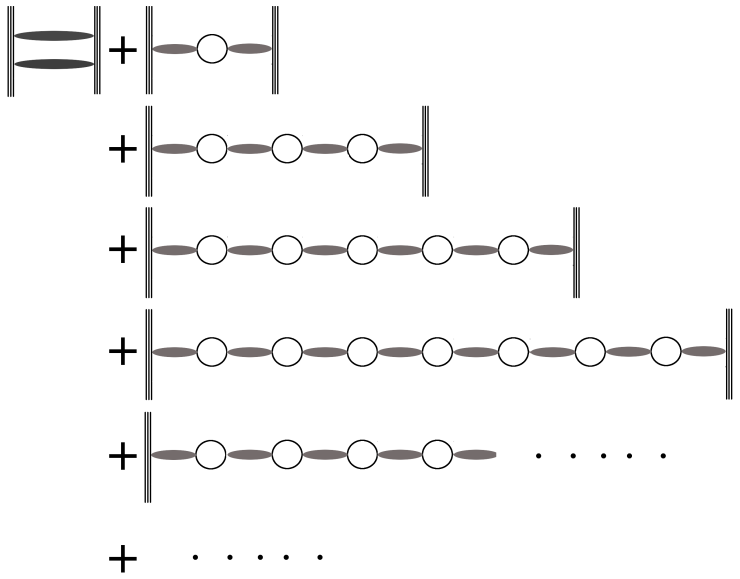

Figure 12-9: Complete elastic scattering amplitude, T. Gluon Bundles term (two bundles because one bundle is anti-symmetric) plus $\sum$ of infinite chains of loops.

If the right hand side of that GB is to have a different color than the left hand side, with the same transverse coordinate, there will then be an extra factor of 2 choices, as it touches the first left hand side loop. And so there would seem to be an extra factor of 2 for choices of the right hand side quark.

Parameters with the entire infinite loop chain and gluon bundle amplitude resulted

in

$$
\begin{aligned}
g &= 6.0 \\
m_{ext} &= 2m_\pi, \quad m_{int} = 12m_\pi \\
\beta_{ext} &= 3.0, \quad \beta_{int} = 1/9 \\
p &= 0.1 \\
\kappa &= 0.000265
\end{aligned}
\tag{12.2}
$$

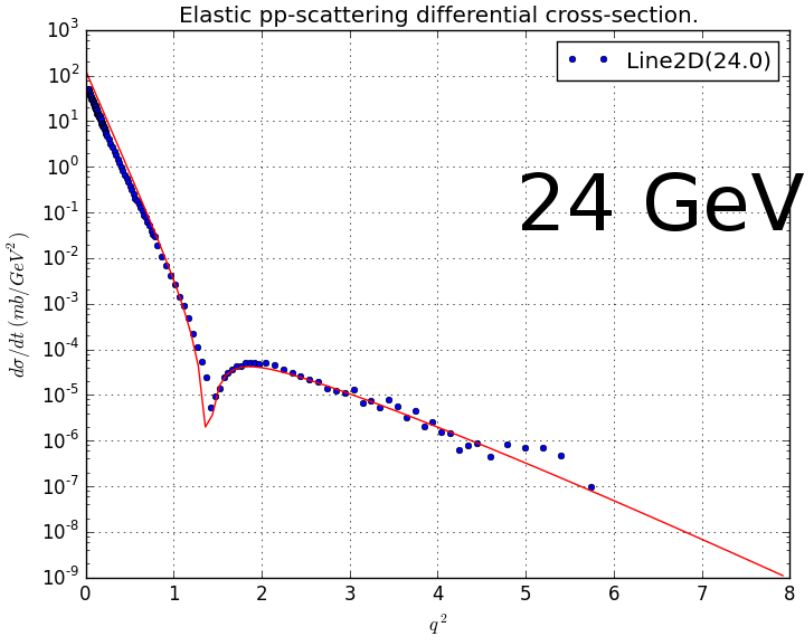

Figure 12-10: 24 GeV ISR fit with infinite loop chains summed.

For LHC's energy of 7 TeV, total cross section should become more relevant.

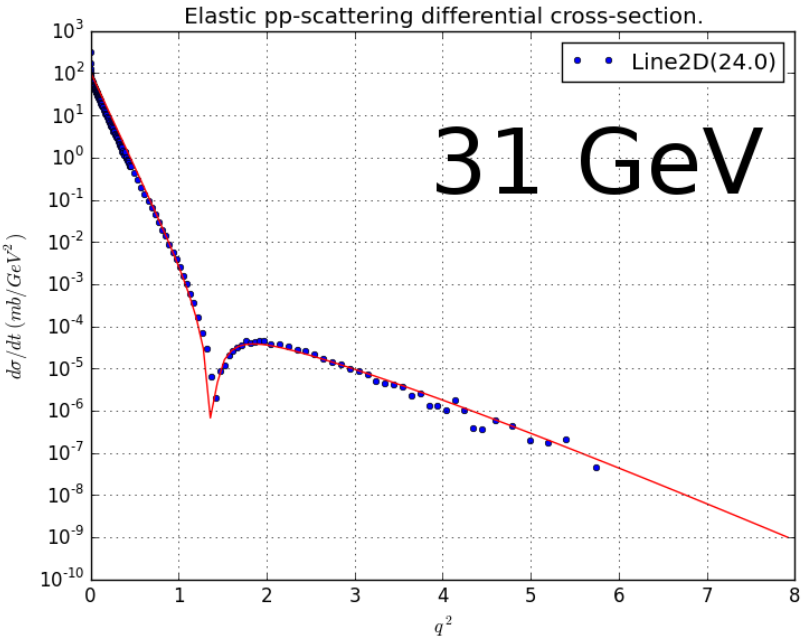

Figure 12-11: 31 GeV ISR fit with infinite loop chains summed.

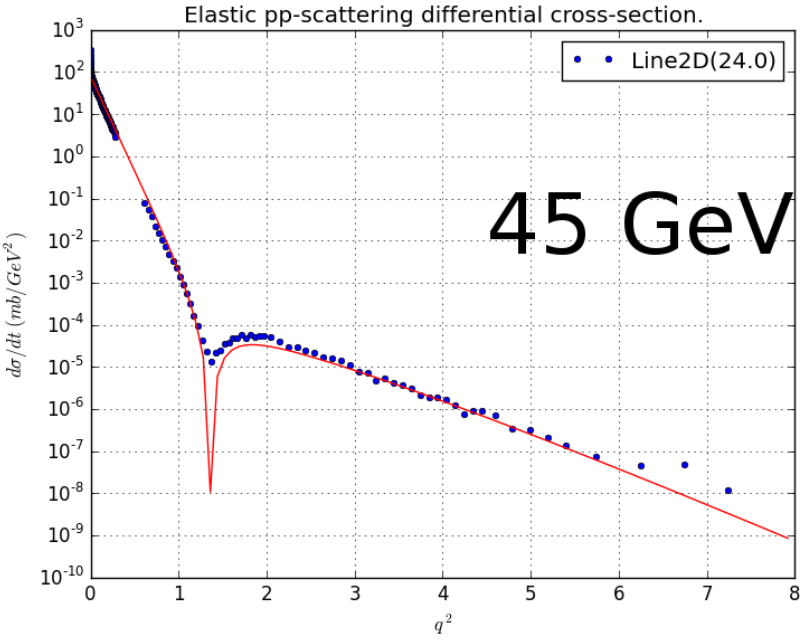

Figure 12-12: 45 GeV ISR fit with infinite loop chains summed.

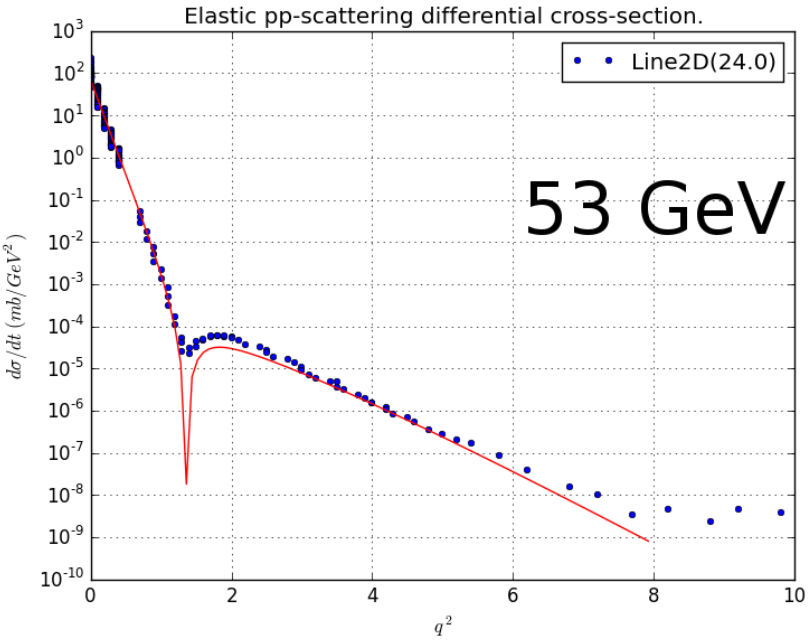

Figure 12-13: 53 GeV ISR fit with infinite loop chains summed.

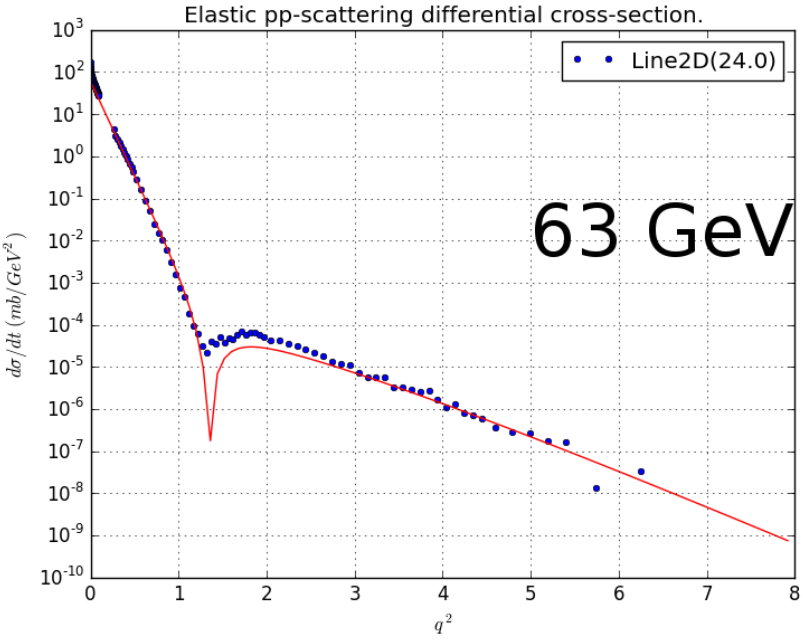

Figure 12-14: 63 GeV ISR fit with infinite loop chains summed.

Chapter 13

Extension to LHC energies and beyond. Summary and Conclusions.

13.1 Total cross section

At 7 TeV and above, we feel it is important to consider to total cross section, σ,

$$\sigma = \frac{4\pi}{k}\mathfrak{Im}[T(0)] \tag{13.1}$$

is proportional to the imaginary part of the foward amplitude, $T(0)$. As first derived by Cheng and Wu in their seminal paper [15], that the cross-section should rise with increasing center of mass energy,

$$ln^2\left(\frac{(s/s_0)^a}{ln^2(s/s_0)}\right) \tag{13.2}$$

and later confirmed by experiments. Data from Totem collaboration at the LHC [18, 19], Figure 13-1 shows that at LHC energies, the total cross-section is much higher than at the ISR energies this report is focused on.

In our renormalization scheme where the δ_q that connects to a physical quark is given the factor $(\frac{m}{E})^{2p}$. Intuitively we feel there should be energy dependence on this p. This work towards the LHC energies is currently underway.

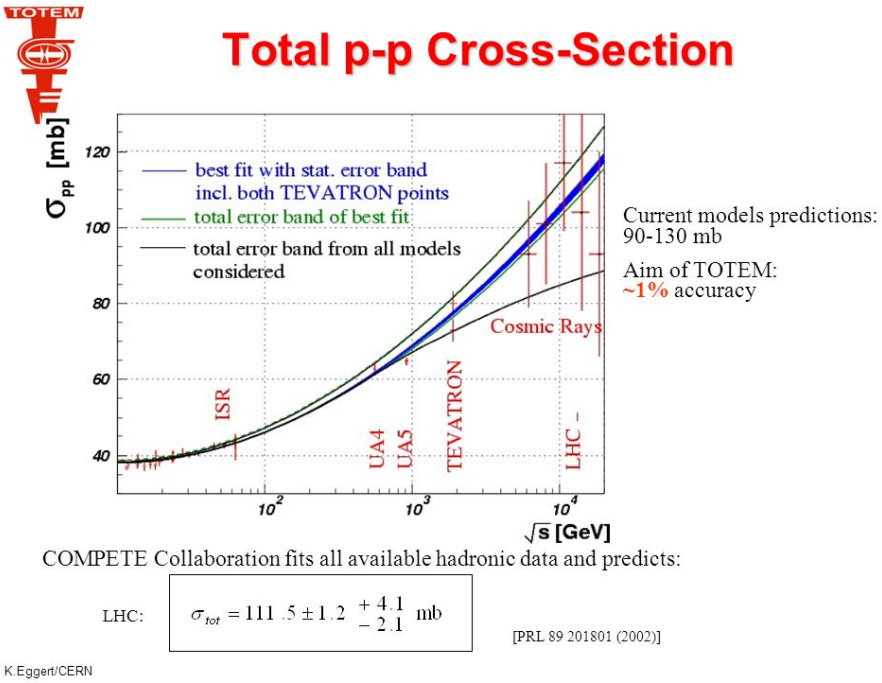

Figure 13-1: Totem's total cross section shows a rise with increasing beam energy.

13.2 Summary and Conclusions

What we have done is began with the Schwinger Action, write down the QCD Lagrangian, imposing that quarks's field must include an imprecision, $\varphi(b)$. From there, through Halpern's Functional in addition to Fradkin's representations, we get explicitly gaussian operations on gaussian integrals. This is possible only in the non-abelian case, which is quite surprising that QCD is perhaps an easier problem than QED. All of the above gives a finite, exact, gauge-invariant, non-perturbative answers to QCD processes and can be done exactly.

1. Gauge invariance is insured in it's strongest form by means of being Gauge-independent.

2. Both Casimir, C_2 and C_3 invariants are preserved.

3. A new property in Effective Locality arose and simplifies all quark/quark processes correlations, without approximation, without exception.

4. Individual gluons have disappeared, giving instead, the entire sum of all gluons

exchanges, a Gluon Bundle.

5. Quark binding is obtained by the vital change of sign in its corresponding potential.

6. The mass of a pion is obtained and in the right order.

7. Nucleon binding, the simplest one in a deuteron is produced.

We, at this point, introduced our particular choice of renormalization where $\delta^2\ell = \kappa$ is assumed finite, we have simplified all loop graphs to simply loop chains. Taking all the SU(3) color fields angles to be of the same order, where $\sum_A \chi^2$ is averaged as R^2, we arrived at elastic scattering amplitudes that we can compare against experiment. Our differential cross-section, with only the coupling constant g, renormalization constants p and κ, and finally the bound state mass factor m_{ext} and m_{int} to be determined from experiments. The results compare remarkably well at ISR energies including energy dependencies that shifts the diffraction dip to lower q^2, and the form of the curve. Certainly, comparison with LHC data is the next logical step and is underway.

We feel, at this stage, this formalism of QCD is on good footing. Perhaps QCD can be raised to the level of QED as a true theory of nature.

Appendix A

Appendix A

A.1 Modified Fradkin's Represenation of Green's function and Closed-Fermion-Loop Functional

The causal Green's function in Eq. (**??**) can be written as [23]

$$\mathbf{G}_c[A] = [m + i\gamma\cdot\Pi][m + (\gamma\cdot\Pi)^2]^{-1} = [m + i\gamma\cdot\Pi]\cdot i\int_0^\infty ds\, e^{-ism^2}\, e^{is(\gamma\cdot\Pi)^2}, \quad \text{(A.1)}$$

where $\Pi = i[\partial_\mu - igA^a_\mu\tau^a]$ and $(\gamma\cdot\Pi)^2 = \Pi^2 + ig\sigma_{\mu\nu}\,\mathbf{F}^a_{\mu\nu}\tau^a$ with $\sigma_{\mu\nu} = \frac{1}{4}[\gamma_\mu,\gamma_\nu]$. Following the Fradkin's method and replacing Π_μ with $i\frac{\delta}{\delta v_\mu}$, one obtains

$$\begin{aligned} & \mathbf{G}_c(x,y|A) \qquad\qquad\qquad\qquad\qquad\qquad\qquad\qquad\qquad\qquad\qquad\qquad \text{(A.2)} \\ = \;& i\int_0^\infty ds\; e^{-ism^2}\cdot e^{i\int_0^s ds'\frac{\delta^2}{\delta v^2_\mu(s')}}\cdot\left[m - \gamma_\mu\,\frac{\delta}{\delta v_\mu(s)}\right]\delta(x - y + \int_0^s ds'\; v(s')) \\ & \times\left(\exp\left\{-ig\int_0^s ds'\left[v_\mu(s')\,A^a_\mu(y - \int_0^{s'} v)\tau^a + i\sigma_{\mu\nu}\,\mathbf{F}^a_{\mu\nu}(y - \int_0^{s'} v)\tau^a\right]\right\}\right)_+\Bigg|_{v_\mu\to 0}. \end{aligned}$$

Then, one can insert [26]

$$1 = \int \mathrm{d}[u]\,\delta(u(s') - \int_0^{s'} ds''\; v(s'')) \qquad\qquad \text{(A.3)}$$

and replace the delta-functional $\delta(u(s') - \int_0^{s'} ds''\; v(s''))$ with a functional integral over

Ω, then the Green's function becomes [59]

$$\begin{aligned}
&\mathbf{G}_c(x,y|A) \qquad\qquad (A.4)\\
&= i\int_0^\infty ds\; e^{-ism^2}\, e^{-\frac{1}{2}\mathrm{Tr}\ln(2h)} \int d[u]\, e^{\frac{i}{4}\int_0^s ds'\,[u'(s')]^2}\,\delta^{(4)}(x-y+u(s))\\
&\quad\times\left[m+ig\gamma_\mu A^a_\mu(y-u(s))\tau^a\right]\,\left(e^{-ig\int_0^s ds'\,u'_\mu(s')\,A^a_\mu(y-u(s'))\,\tau^a+g\int_0^s ds'\sigma_{\mu\nu}\,\mathbf{F}^a_{\mu\nu}(y-u(s'))\,\tau^a}\right)_+,
\end{aligned}$$

where $h(s_1,s_2)=\int_0^s ds'\,\theta(s_1-s')\theta(s_2-s')$. To remove the A^a_μ-dependence out of the linear (mass) term, one can replace $igA^a_\mu(y-u(s))\tau^a$ with $-\frac{\delta}{\delta u'_\mu(s)}$ operating on the ordered exponential so that

$$\begin{aligned}
\mathbf{G}_c(x,y|A) &= i\int_0^\infty ds\; e^{-ism^2}\, e^{-\frac{1}{2}\mathrm{Tr}\ln(2h)} \int d[u]\, e^{\frac{i}{4}\int_0^s ds'\,[u'(s')]^2}\,\delta^{(4)}(x-y+u(s)) \qquad (A.5)\\
&\quad\times\left[m-\gamma_\mu\frac{\delta}{\delta u'_\mu(s)}\right]\,\left(e^{-ig\int_0^s ds'\,u'_\mu(s')\,A^a_\mu(y-u(s'))\,\tau^a+g\int_0^s ds'\sigma_{\mu\nu}\,\mathbf{F}^a_{\mu\nu}(y-u(s'))\,\tau^a}\right)_+.
\end{aligned}$$

To extract the A-dependence out of the ordered exponential, one may use the identities

$$\begin{aligned}
1 &= \int d[\alpha]\,\delta\left[\alpha^a(s')+gu'_\mu(s')\,A^a_\mu(y-u(s'))\right] \qquad (A.6)\\
1 &= \int d[\Xi]\,\delta\left[\Xi^a_{\mu\nu}(s')-g\mathbf{F}^a_{\mu\nu}(y-u(s'))\right]
\end{aligned}$$

so that

$$\begin{aligned}
&\left(e^{-ig\int_0^s ds'\,u'_\mu(s')\,A^a_\mu(y-u(s'))\,\tau^a+g\int_0^s ds'\sigma_{\mu\nu}\,\mathbf{F}^a_{\mu\nu}(y-u(s'))\,\tau^a}\right)_+ \qquad (A.7)\\
&= \mathcal{N}_\Omega\mathcal{N}_\Phi\int d[\alpha]\int d[\Xi]\int d[\Omega]\int d[\mathbf{\Phi}]\,\left(e^{i\int_0^s ds'\left[\alpha^a(s')-i\sigma_{\mu\nu}\,\Xi^a_{\mu\nu}(s')\right]\tau^a}\right)_+\\
&\quad\times e^{-i\int ds'\,\Omega^a(s')\,\alpha^a(s')-i\int ds'\,\mathbf{\Phi}^a_{\mu\nu}(s')\,\Xi^a_{\mu\nu}(s')}\\
&\quad\times e^{-ig\int ds'\,u'_\mu(s')\,\Omega^a(s')\,A^a_\mu(y-u(s'))+ig\int ds'\,\mathbf{\Phi}^a_{\mu\nu}(s')\,\mathbf{F}^a_{\mu\nu}(y-u(s'))},
\end{aligned}$$

where $\mathcal{N}_\Omega$ and $\mathcal{N}_\Phi$ are constants which normalize the functional representations of the delta-functionals. All A-dependence is removed from the ordered exponentials and the resulting form of the Green's function is exact (it entails no approximation).

Alternatively, extracting the A-dependence out of the ordered exponential can also be achieved by using the functional translation operator. One writes

$$\left(e^{+g\int_0^s ds'\left[\sigma_{\mu\nu}\,\mathbf{F}^a_{\mu\nu}(y-u(s'))\tau^a\right]}\right)_+ = e^{g\int_0^s ds'\,\mathbf{F}^a_{\mu\nu}(y-u(s'))\,\frac{\delta}{\delta\mathbf{\Xi}^a_{\mu\nu}(s')}}\cdot\left(e^{\int_0^s ds'\left[\sigma_{\mu\nu}\,\mathbf{\Xi}^a_{\mu\nu}(s')\tau^a\right]}\right)_+\Bigg|_{\mathbf{\Xi}\to 0}. \tag{A.8}$$

For the closed-fermion-loop functional $\mathbf{L}[A]$, one can write [23]

$$\mathbf{L}[A] = -\frac{1}{2}\int_0^\infty \frac{ds}{s}\,e^{-ism^2}\,\Big\{\mathrm{Tr}\left[e^{-is(\gamma\cdot\Pi)^2}\right] - \{g=0\}\Big\}, \tag{A.9}$$

where the trace sums over all degrees of freedom. The Fradkin's representation proceeds along the same steps as in the case of $\mathbf{G}_c[A]$, and the closed-fermion-loop functional reads

$$\begin{aligned}\mathbf{L}[A] \;=\; & -\frac{1}{2}\int_0^\infty \frac{ds}{s}\,e^{-ism^2}\,e^{-\frac{1}{2}\mathrm{Tr}\ln(2h)} \\ & \times\int d[v]\,\delta^{(4)}(v(s))\,e^{\frac{i}{4}\int_0^s ds'\,[v'(s')]^2} \\ & \times\int d^4x\,\mathrm{tr}\left(e^{-ig\int_0^s ds'\,v'_\mu(s')\,A^a_\mu(x-v(s'))\,\tau^a + g\int_0^s ds'\sigma_{\mu\nu}\,\mathbf{F}^a_{\mu\nu}(x-v(s'))\,\tau^a}\right)_+ \\ & -\{g=0\}\,,\end{aligned} \tag{A.10}$$

where the trace now sums over color and spinor indices. Also, Fradkin's variables have been denoted by $v(s')$, instead of $u(s')$, in order to distinguish them from those

appearing in the Green's function $\mathbf{G}_c[A]$. One finds

$$
\begin{aligned}
\mathbf{L}[A] \;=\; & -\frac{1}{2}\int_0^\infty \frac{ds}{s}\, e^{-ism^2}\, e^{-\frac{1}{2}\mathrm{Tr}\ln(2h)} \\
& \times \mathcal{N}_\Omega \mathcal{N}_\Phi \int d^4x \int \mathrm{d}[\alpha] \int \mathrm{d}[\Omega] \int \mathrm{d}[\boldsymbol{\Xi}] \int \mathrm{d}[\boldsymbol{\Phi}] \\
& \times \int d[v]\, \delta^{(4)}\big(v(s)\big)\, e^{\frac{i}{4}\int_0^s ds'\,[v'(s')]^2} \\
& \times\; e^{-i\int ds'\,\Omega^a(s')\,\alpha^a(s') - i\int ds'\,\boldsymbol{\Phi}^a_{\mu\nu}(s')\,\boldsymbol{\Xi}^a_{\mu\nu}(s')} \cdot \mathrm{tr}\left(e^{i\int_0^s ds'\left[\alpha^a(s') - i\sigma_{\mu\nu}\,\boldsymbol{\Xi}^a_{\mu\nu}(s')\right]\tau^a}\right)_+ \\
& \times e^{-ig\int_0^s ds'\,v'_\mu(s')\,\Omega^a(s')\,A^a_\mu(x-v(s')) - 2ig\int d^4z\left(\partial_\nu \boldsymbol{\Phi}^a_{\nu\mu}(z)\right)A^a_\mu(z)} \\
& \times e^{+ig^2\int ds'\, f^{abc}\boldsymbol{\Phi}^a_{\mu\nu}(s')\,A^b_\mu(x-v(s'))\,A^c_\nu(x-v(s'))} \\
& -\{g=0\}\,,
\end{aligned}
\tag{A.11}
$$

where the same properties as those of $\mathbf{G}_c[A]$ can be read off explicitly and the A-dependence is at most Gaussian.

Appendix B

Appendix B

Hadron	m_{BS} $[GeV/c^2]$	Quark Content	x	ξ
Proton	0.938	uud	6.7	0.05
Neutron	0.939	udd	6.7	0.05
Lambda,Λ^0	1.116	uds	8.0	0.04
Charmed Lambda, Λ_c^+	2.286	udc	16.3	0.009
bottom Lambda, Λ_b^0	5.619	udb	40.1	0.008
Sigma+, Σ^+	1.189	uus	8.5	0.03
Sigma0, Σ^0	1.193	uds	8.5	0.03
Sigma-, Σ^-	1.197	dds	8.6	0.03
Charmed Sigma, Σ_c^{++}	2.454	uuc	17.5	0.009
Bottom Sigma, Σ_b^+	5.811	uub	41.5	0.008
Bottom Sigma, Σ_b^-	5.816	ddb	41.5	0.008
Xi, Ξ^0	1.315	uss	9.4	0.03
Xi, Ξ^-	1.322	dss	9.4	0.03
Charmed Xi, Ξ_c^+	2.468	usc	17.6	0.008
charmed Xi, Ξ_c^0	2.471	dsc	17.6	0.008
charmed Xi prime, $\Xi_c^{\prime +}$	2.575	usc	18.4	0.008
charmed Xi prime, $\Xi_c^{\prime 0}$	2.578	dsc	18.4	0.008
double charmed Xi, Ξ_{cc}^+	3.519	dcc	25.1	0.004

bottom Xi (Cascade B), Ξ_b^0	5.788	usb	41.3	0.008
bottom Xi(Cascade B), Ξ_b^-	5.791	dsb	41.4	0.008
charmed Omega, Ω_c^0	2.695	ssc	19.3	0.008
bottom Omega, Ω_b^-	6.071	ssb	43.4	0.007

Table B.1: ξ-values for the known hadrons, using correct quark flavor masses [**?**], displays the expected variations in ξ as a function of x where $x = m_{BS}/m_\pi$

Figure B-1: QCD Confinement scales.

Figure B-2: QCD confinement scales.

Bibliography

[1] L.F. Alday and Juan. Maldacena. Gluon scattering amplitudes at strong coupling. *JHEP*, 2007, 2007.

[2] U Amaldi and K.R. Schubert. *Nucl. Phys. B*, 166:301, 1980.

[3] M Ambrosio, (CERN-Naples-Pisa-Stony Brook Collaboration), et al. *Phys. Lett. B*, 115:495, 1982.

[4] N.A. Amos et al. *Nucl. Phys. B*, 262:689, 1985.

[5] I.I. Balitsky and L.N. Lipatov. *Sov. J. Nucl. Phys.*, 28:822, 1978.

[6] I.I. Balitsky and L.N. Lipatov. *JETP Lett.*, 30:355, 1979.

[7] Z. Bern, L. J. Dixon, and V.A. Smirnov. Iteration of planar amplitudes in maximally supersymmetric yang-mills theory at three loops and beyond. *Phys. Rev. D*, 72:085001, 2005.

[8] A Breakstone, (Ames Bologna CERN Dortmund Heidelberg Warsaw Collaboration), et al. Charged multiplicity distribution in pp interactions at cern isr energies, 1984.

[9] S.J. Brodsky. Perspectives and challenges for qcd phenomenology. In *APS/DPF/DPB Summer Study On the Future Of Particle Physics*, Snowmass, Colorado, 2001. APS/DPF/DPB.

[10] S.J. Brodsky, G.F. de Teramond, H.G. Dosch, and J. Erlich. Light-front holographic qcd and emerging confinement. *Physics Reports*, 583:1–105, 2015. arXiv 1407.8131v2.

[11] S.J. Brodsky, G.F. Teramond, and H.G. Dosch. Threefold complementary approach to holographic qcd. *Phys. Lett. B*, 729, 2014.

[12] R.C. Brower, J. Polchinski, M.J. Strassler, and C.-I. Tan. The pomeron and gauge/string duality. *JHEP12*, 2007, 2007.

[13] R.C. Brower, J. Polchinski, M.J. Strassler, and C.-I. Tan. On the eikonal approximation in ads space. *JHEP*, 2009.

[14] R.C. Brower, M.J. Strassler, and C.-I. Tan. On the pomeron at large t'hooft coupling. *JHEP*, 2009.

[15] H. Cheng and T.T. Wu. Limit of cross sections at infinite energy. *Phys. Rev. Lett.*, 24:1456, 1970.

[16] A Donnachie and P.V. Landshoff. pp and p$\bar{p}$ total cross-sections and elastic scattering. *Phys. Lett. B*, 727:500–505, 2013.

[17] E Eichen, K. Gottfried, T. Kinoshita, K.D. Lane, and T.-M Yan. Charmonium: The model. *Phys. Rev. D*, 17:3090, 1978.

[18] The TOTEM Collaboration *et al. Eur. Phys. Lett.*, 95:41001, 2011.

[19] The TOTEM Collaboration *et al. Eur. Phys. Lett.*, 101:21002, 2013. doi: 10.1209/0295-5075/101/21002.

[20] V.S. Fadin, E.A. E. A. Kuraev, and L.N. Lipatov. *Phys. Lett. B*, 60:50, 1975.

[21] E.S. Fradkin. *Dokl. Akad. Nauk. SSSR*, 98:47, 1954.

[22] E.S. Fradkin. *Nucl. Phys.*, 76:588–624, 1966.

[23] H.M. Fried. *Basics of Functional Methods and Eikonal Models*. Editions Frontiéres, Gif-sur-Yvette Cedex, France, 1990.

[24] H.M. Fried. A new, analytic, non-perturbative, gauge-invariant, realistic formulation of qcd. *Modern Phys. Letts.*, A 28:1230045, 2013.

[25] H.M. Fried and Y. Gabellini. On the summation of feynman graphs. *Ann. Phys.*, 327:1645–1667, 2012.

[26] H.M. Fried, Y. Gabellini, T. Grandou, and Y.-M. Sheu. Gauge invariant summation of all qcd virtual gluon exchanges. *Eur. Phys. J. C*, 65:395–411, 2010. arXiv:0903.2644v2.

[27] H.M. Fried, Y. Gabellini, T Grandou, and Y.-M. Sheu. Analytic qcd binding potentials. *arXiv:1104.4663*, 2011.

[28] H.M. Fried, Y Gabellini, T Grandou, and Y.-M. Sheu. Analytic, non-perturbative, gauge-invariant qcd: Nucleon scattering and binding potentials. *Ann.Phys.*, 338:107–122, 2013.

[29] H.M. Fried, M Gattobigio, T Grandou, and Y.-M. Sheu. On qcd and effective locality. *AIP Conf. Proc.*, 2011.

[30] H.M. Fried, T. Grandou, and Y.-M. Sheu. A new approach to analytic, non-perturbative and gauge-invariant qcd. *Ann.Phys.*, 327:2666–2690, 2012.

[31] H.M. Fried, T. Grandou, and Y.-M. Sheu. Non-perturbative qcd amplitudes in quenched and eikonal approximations. *Ann. of Phys.*, 344:78–96, 2014. arXiv:1207.5017v3.

[32] H.M. Fried and P.H. Tsang. A physical version of the qcd confinement scale(s). *arXiv:1502.04378*, 2015.

[33] H.M. Fried, P.H. Tsang, Y Gabellini, T Grandou, and Y.-M. Sheu. An exact, finite, gauge-invariant, non-perturbative model of qcd renormalization. *Ann. Phys.*, 359:1–19, 2015. arXiv:1412.2072.

[34] T. Grandou. On the casimir operator dependences of qcd amplitudes. *Eur. Phys. Lett.*, 107:11001, 2014. arXiv:1402.7273 [hep-th].

[35] T. Grandou, H.M. Fried, and R. Hofman. Casimir operator dependences of non-perturbative fermionic qcd amplitudes. *arXiv:1504.05502[hep-th]*, 2015.

[36] V.N. Gribov and L.N. Lipatov. *Sov. J. Nucl. Phys.*, 15:438, 1972.

[37] D.J. Gross and F. Wilczek. Ultraviolet behavior of non-abelian gauge theories. *Phys. Rev. Lett.*, 30, 1973.

[38] M.B. Halpern. Field-strength formulation of quantum chromodynamics. *Phys. Rev. D*, 16(6):1798, 1977.

[39] M.B. Halpern. Gauge-invariant formulation of the self-dual sector*. *Phys. Rev. D*, 16(12):3515, 1977.

[40] Arthur Jaffe and Edward Witten. Quantum yang-mills theory. *Clay Mathematics Institute, Millennium Problems.*

[41] I.A. Korzhavina, H1, and ZEUS collaborations. Diffractive structure functions from h1 and zeus experiments at hera.

[42] E.A. Kuraev and L. N. Lipatov. *Sov. Phys. JETP*, 45:199, 1977.

[43] E.A. Kuraev, L.N. Lipatov, and V.S. Fadin. *Sov. Phys. JETP*, 44:443, 1976.

[44] L.N. Lipatov. *Sov. J. Nucl. Phys.*, 23:338, 1976.

[45] L.N. Lipatov. Reggeization of the vector meson and the vacuum singularity in nonabelian gauge theories. *Sov. J. Nucl. Phys.*, 23:338, 1976.

[46] L.N. Lipatov. *Sov. Phys. JETP*, 63:904, 1986.

[47] L.N. Lipatov. Integrability of scattering amplitudes in N=4 SUSY. *J. Phys. A*, 42, 2009.

[48] V. Alfaro, S. Fubini, and G. Furlan. Conformal invariance in quantum mechanics. *Nuovo Cim.*, 1976.

[49] G.F. Teramond and S.J. Brodsky. Hadronic form factor models and spectroscopy within the gauge/gravity correspondence. *Invited lectures presented by GdT at the Niccolo Cabeo International School of Hadronic Physics, Ferrara, Italy, May 2011*, 2012.

[50] L. O'Raifeartaigh. *The Dawning of Gauge Theory.* Princeton University Press, 1997.

[51] H.C. Pauli and S.J. Brodsky. Discretized light cone quantization: solution to a field theory in one space time dimensions. *Phys. Rev. D*, 32, 1985.

[52] H.C. Pauli and S.J. Brodsky. Solving field theory in one space time dimension. *Phys. Rev. D*, 32, 1985.

[53] Martin L. Perl. *High Energy Hadron Physics.* Wiley-Interscience, 1974.

[54] H.D. Politzer. Reliable perturbative results for strong interactions? *Phys. Rev. Lett. 30*, 1973.

[55] G.M. Prosperi, M. Raciti, and C. Simolo. On the running coupling constant in qcd. *Prog. Part. Nucl. Phys.*, 58, 2007.

[56] C. Royon, L. Schoeffel, R. Peschanski, and E. Sauvan. Pomeron structure functions from hera to tevatron and lhc. *Nucl. Phys. B*, 746:15, 2006.

[57] G.P. SALAM. An introduction to leading and next-to-leading bfkl. *Acta. Phys. Polon. B*, 30:3679–3705, 1999.

[58] J. Schwinger. On the green's functions of quantized fields. i. *Proceedings of the National Academy of Sciences*, 37:452, 1951.

[59] Y.-M Sheu. *Finite-Temperature QED: General Theory and Bloch-Nordsieck Estimates of Fermion Damping in a Hot Medium.* PhD dissertation, Brown University, Department of Physics, May 2008.

[60] A.P Trawinski, S.D Glazek, S.J. Brodsky, G.F. Teramond, and H.G. Dosch. Effective confining potentials for qcd. *Phys. Rev. D*, 90, 2014.

[61] C.N. Yang and R.L. Mills. Conservation of isotropic spin and isotopic gauge invariance. *Phys. Rev.*, 96:191–195, 1954.

[62] F.J. Yndurain. *Quantum Chromodynamics.* Texts and Monographs in Physics. Springer-Verlag, 1983.